

3. MATERIALS FOR EXHAUST AFTERTREATMENT

A. Materials for Exhaust Aftertreatment

*Paul W. Park, Alexander G. Panov, and Craig F. Habeger
Caterpillar Inc.
P.O. Box 1875
Peoria, IL 61656
(309) 578-4065; fax: (309) 578-2953; e-mail: park_paul_w@cat.com*

*DOE Technology Development Area Specialist: Dr. Sidney Diamond
(202) 586-8032; fax: (202) 586-2476; e-mail: sid.diamond@ee.doe.gov
ORNL Technical Advisor: D. Ray Johnson
(865) 576-6832; fax: (865) 574-6098; e-mail: johnsondr@ornl.gov*

*Contractor: Oak Ridge National Laboratory, Oak Ridge, Tennessee
Prime Contract No: DE-AC05-00OR22725
Subcontractor: Caterpillar Inc., Peoria, Illinois*

Objectives

- Develop advanced materials for diesel engine aftertreatment systems that will comply with future emission regulations.
- Determine the durability of a lean nitrogen oxide (NO_x) catalyst in the presence of sulfur.
- Evaluate the filtration properties of sintered metal particulate filters.
- Complete construction of a designated NO_x sensor analytical bench.
- Evaluate current NO_x sensor technologies.

Approach

- Identify ideal combinations of catalyst materials and specific fuel-born hydrocarbon reductants that will demonstrate higher NO_x reduction than the state-of-the-art lean-NO_x catalyst materials.
- Understand and improve catalyst durability with regard to sulfur poisoning and thermal degradation by characterizing catalyst materials thoroughly and synthesizing more durable catalyst formulations.
- Develop full scale-up catalyst bricks by developing a washcoat technique in-house.
- Synthesize sensor electrode materials.
- Fabricate particulate filters or NO_x sensors.
- Acquire an externally derived catalyst, NO_x sensor, or particulate trap.
- Evaluate the performance of the catalyst, NO_x sensor, or particulate trap.

Accomplishments

- Identified a promising catalyst combination for a specific reductant.
- Developed an understanding of the sulfur poisoning mechanism on silver-doped alumina catalysts.
- Identified active sites on silver-doped alumina catalysts.
- Developed test protocols to evaluate catalysts using various liquid hydrocarbons.
- Washcoated full-size brick (10.5 × 6 in.) for engine tests.
- Completed the NO_x sensor bench.
- Developed agreements with NO_x sensor developers to evaluate their sensors.

Future Direction

- Understand the synergy effect from a combination of catalyst material and a reductant choice.
- Develop catalyst formulations to improve NO_x performance.
- Improve the washcoat technique to prepare full-size engine tests.
- Assess the feasibility of selected hydrocarbons for real application.
- Evaluate NO_x sensor electrodes and adjust them as needed.

Introduction

The objective of this effort is to develop and evaluate materials that will be used in aftertreatment systems for diesel engines. These materials include catalysts for NO_x abatement, filtration media for particulate abatement, and materials to improve NO_x sensing capabilities in the exhaust system. This project is part of a Caterpillar strategy to meet U.S. Environmental Protection Agency (EPA) requirements for regulated emissions in 2007 and beyond. This year's focus is on the durability of NO_x catalysts developed for lean burn applications in the presence of sulfur, evaluation of filtration properties of sintered metal media for application in diesel particulate filters, and evaluation of current NO_x sensor technologies while developing materials to improve sensing capabilities.

Approach

Lean NO_x

The study of SO₂ durability of silver catalysts study focused on understanding

catalyst durability with regard to sulfur poisoning. The catalyst performance was evaluated using NO_x (NO or NO₂) with SO₂ on a powder bench test system. The catalyst samples were characterized by diffuse reflectance infrared Fourier transform spectroscopy (DRIFT) to determine surface species, and by a sulfur analyzer to quantify sulfur content in the samples.

The effect of various alcohols (ethanol, propanol, butanol, hexanol, octanol), liquid hydrocarbons (octane, dodecane, and hexadecane) and various fuels (2 ppm sulfur diesel; 8 ppm sulfur diesel; 500 ppm sulfur diesel, gasoline, and kerosene) on the performance of lean NO_x catalysts has been examined with powder samples and 1×3 in. washcoated honeycomb monolith samples.

NO_x Sensor

In order to develop and evaluate NO_x sensors, a dedicated analytical bench is necessary. Work was performed to construct evaluation facilities. The reactor bench principle is to flow reaction gas over the

sensor and measure the sensor response. The reaction gas is mixed in the desired proportions using the starting compressed gas cylinder concentrations and the mass flow controllers. Once built, the test bench will be used to evaluate sensors from other developers, along with sensing electrode materials that have been synthesized internally at Caterpillar.

Particulate Matter Trap

Particulate filters have been evaluated using the diesel fuel burner. The methodology to evaluate filtration efficiency and pressure drop was refined. Sintered metal filters were also prepared. Sintered metal filters, sintered metal fiber filters, and catalyzed filters were evaluated.

Results

Lean NO_x

SO₂ durability of silver catalysts. The study showed that SO₂ did not permanently poison the silver catalysts but promoted NO reduction performance under certain conditions. The initial increase in N₂ yield suggests that the silver sulfate phase is active for NO reduction. The decrease in activity after long exposure to SO₂ is due to the sulfation of the alumina support. Figure 1 shows the comparison of NO reduction over 2 wt % silver catalysts prepared with sulfate and nitrate precursors. The silver catalyst prepared with silver sulfate compound contained 0.22 wt % sulfur in the sample; however, it showed higher catalytic performance for NO reduction than the sample prepared with silver nitrate. The catalyst performance and characterization results indicate that the silver sulfate phase has similar or higher catalytic activity, compared with silver oxide species, for NO_x reduction. The order of catalytic activity for NO_x reduction for silver species is proposed as follows: Ag₂SO₄ ≥ Ag₂O >> Ag.

Mesoporous alumina material synthesis. A method for preparing high-

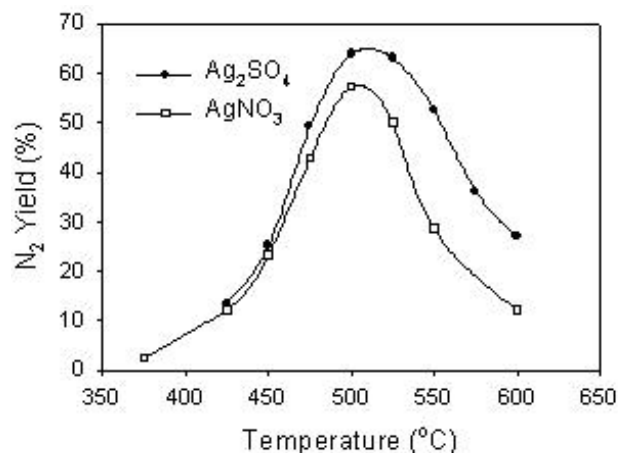


Figure 1. Effect of silver precursors on NO reduction over 2 wt % Ag/Al₂O₃ catalysts (0.1% NO, 0.1% propene, 9% O₂, 7% H₂O, 30,000 h⁻¹)

surface-area mesoporous aluminas was developed using various structure-directing agents. Characterization showed that the mesoporous aluminas have a surface area of up to 580 m²/g and pore volume of up to 1.8 cm³/g. (Surface area and pore volume were identified in the previous year as key properties of the alumina support material for lean-NO_x catalysis.) Based on the combined surface area, X-ray, small angle X-ray scattering, and transmission electron microscopy data, the mesoporous alumina can be described as sponge-like materials with an interpenetrating pore network (see Figure 2). The pore structure is a great advantage because the pore network is accessible for reactive species from any external surface. The mesoporous alumina developed by Caterpillar is a prospective support material for NO_x/SO_x traps or absorbers and NO_x sensors, as well as catalyst support. Future work will be focused on the development of high-surface-area and high-thermal-stability (up to 700°C) mesoporous alumina.

Lean NO_x. The effect of various alcohols (ethanol, propanol, butanol, hexanol, octanol), liquid hydrocarbons (octane, dodecane and hexadecane) and various fuels (2 ppm sulfur diesel, 8 ppm sulfur diesel,

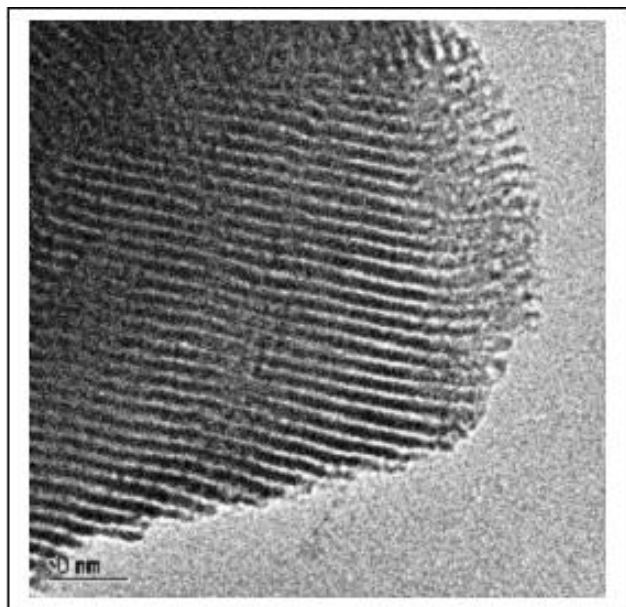


Figure 2. Transmission electron micrograph of mesoporous alumina.

500 ppm sulfur diesel, gasoline and kerosene) on the performance of lean NO_x catalysts has been examined using powder catalyst samples and 1×3 in. washcoated honeycomb monolith samples. The results showed that ethanol had the highest NO_x reduction among the tested alcohols (90% NO_x conversion, 350–400EC, 30,000 h^{-1}). The high-hydrocarbon-chain alcohols, which may be more feasible for real applications than ethanol, also showed promising NO_x conversion (60–70%) at low temperatures (300–375EC). Dodecane reductant also showed promising NO_x reduction among the tested hydrocarbons (40% NO_x conversion, 400EC, 50,000 h^{-1}). A series of catalyst samples prepared with various silver loadings and preparation techniques were evaluated in order to optimize catalyst formulation for different reductants. The relationship between catalyst formulation and reductant species will be further examined to achieve higher NO_x conversion with minimum hydrocarbon consumption.

Test facilities. A new test protocol was developed to evaluate catalyst materials using liquid hydrocarbon reductants on the powder bench system. The effects of various

hydrocarbons on the performance of lean NO_x catalyst can be examined with the developed test protocol. Also, the installation of the multi-reactor catalyst test bench system has been completed. This multi-reactor system (Figure 3) will provide high-throughput screening of catalyst materials in both powder and washcoated-core samples for various catalyst aftertreatment technologies, including oxidation, ammonia selective catalyst reduction, lean- NO_x , and NO_x -trap.

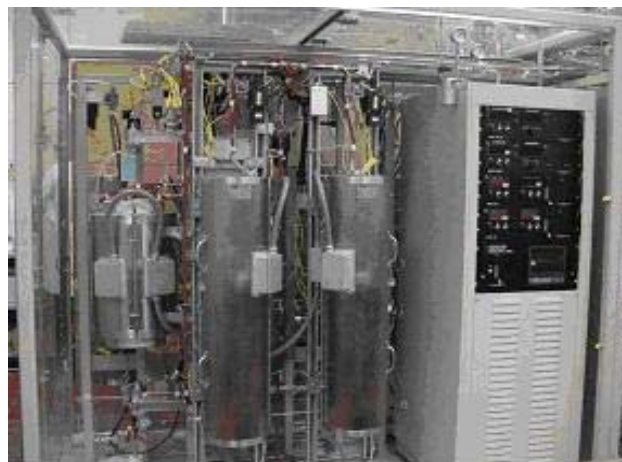


Figure 3. The multi-reactor catalyst test system.

NO_x Sensor

The test bench gas composition can be controlled over a wide range to simulate real diesel exhaust compositions. The flow rate of gas can be varied from 5800 sccm. The low flow rate is important in performing sensor development, initial evaluation, and more fundamental studies. The temperature of the gas or reactor can span the range from ambient to 1000EC to evaluate the effects of temperature.

The test bench shown in Figure 4 is predominately computer controlled. It was designed to be versatile yet easy to use. The computer using Labview software controls the mass flow controllers and all the valves. The aspects of the test bench that are not yet computer controlled are the furnace control and the data acquisition. The graphical user interface (Figure 5) of the test program is

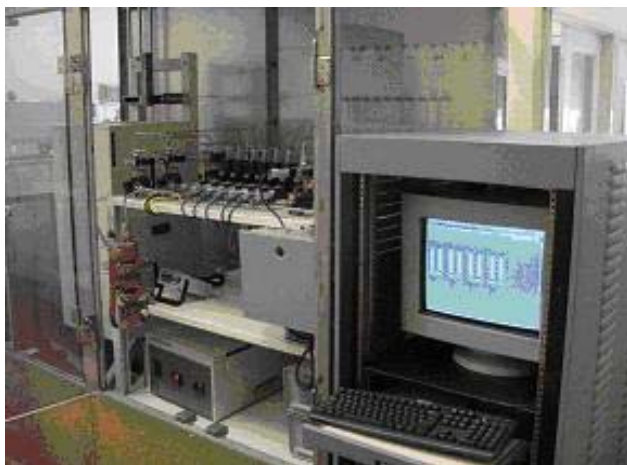


Figure 4. The NO_x sensor bench is a versatile tool for evaluating a broad range of sensing technologies.



Figure 5. The control screen is simple and easy to understand, as shown in this picture of the NO_x sensor test bench control screen.

intuitive and easily operated. As can be seen from Figure 5, the choice of each gas is available for testing. The user can adjust the flow rates by filling in the desired flow rate or toggling up the number to the preferred rate. The user can also change the flow paths by toggling between high flow/low flow, no water/water, to analyzer/to reactor, or "u" reactor/through reactor. In all cases, one toggle click will adjust all the necessary valves to alter the flow path correctly

This program also involves acquiring NO_x sensors from outside developers. Currently, we possess four sensors that are being developed by outside parties. Two of those sensors are based on the mixed potential measurement technique, one is an amperometric sensor, and one is potentiometric.

Current amperometric-type NO_x sensors have deficiencies associated with their multiple electrode designs. The electrodes are optimized for specific performance characteristics; however, when they are optimized for specific performance, a loss in durability appears to result. Work to develop the oxygen-pumping electrode in amperometric sensors was undertaken, keeping in mind performance and durability. Various electrode materials have been synthesized and processed into lab sensor structures for evaluation of performance.

PM Trap

In collaboration with Kyeong Lee at Argonne National Laboratory, the soot from the diesel fuel burner exhaust was collected and evaluated by transmission electron microscopy. The results are not yet available.

Preparation and filtration properties of sintered powder metal filters were studied in detail. It was determined that for the filters prepared from water-atomized metal powder, the transition from surface to deep-bed soot filtration occurs when the pore size reaches about 30 μm , as demonstrated in Figure 6.

Early attempts to make a sintered powder metal filter from an FeCrAl alloy using a binder technique were unsuccessful. We believe the presence of binder complicates sintering. In the future, a binder-free method of preparation will be evaluated.

The soot filtration performance of sintered metal fiber filters has also been studied. Increasing the thickness of the filtration media while keeping the density of the filter relatively low is effective in achieving a high filtration efficiency while maintaining low backpressure.

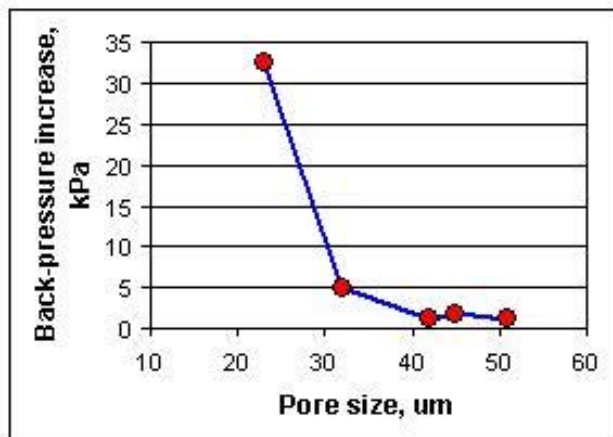


Figure 6. Backpressure increase for sintered powder metal filters loaded with soot.

During the last year, we have also started work on catalyzed soot filters. Currently, we are developing a test procedure to characterize the soot oxidation capability of different catalytic technologies. The activation energy of soot oxidation by NO_2 was determined for two cordierite wall-flow diesel particulate filters (DPFs), as shown in Figure 7. Catalyzed and uncatalyzed DPF

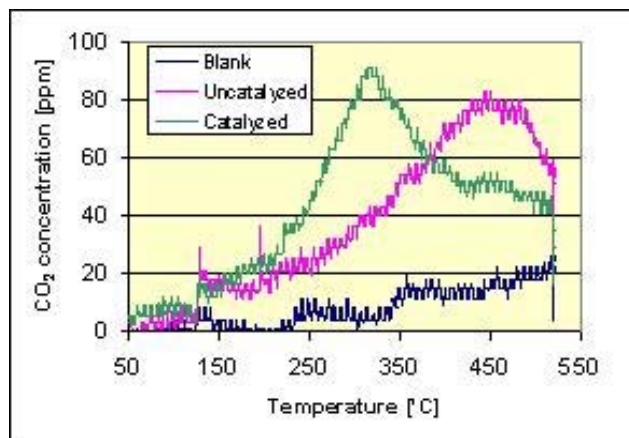


Figure 7. CO_2 evolution during regeneration of catalyzed and uncatalyzed cordierite wall-flow DPFs. Gas composition: NO_2 , 500 ppm; O_2 , 10%; H_2O , 6%.

substrates were tested. An uncatalyzed substrate was used to simulate a continuously regenerating technology type of DPF configuration. The activation energy for catalyzed and uncatalyzed filters was

found to be 107.5 and 160 kJ/mol, respectively. The values of activation energy correlate well with the published data. Activation energy data suggest that catalyzing the DPF is more advantageous for soot oxidation than is placing the oxidation catalyst upstream of an uncatalyzed filter.

In addition, a catalyst coating for the metal and ceramic substrates is being developed. The work will lead to development of a deep-bed catalyzed particulate filter that should have higher NO_x turnover frequency. Higher NO_x turnover frequency, theoretically, should result in higher soot oxidation rates than are obtained with typical wall-flow DPF materials.

Conclusions

This research has shown that important catalyst breakthroughs are being made with regard to lean NO_x catalysis. Capabilities to perform and decrease the evaluation time of catalysts, NO_x sensors and PM traps have been developed at Caterpillar. These tools are being used to develop state-of-the-art materials and evaluate such materials developed elsewhere.

Publications/Presentations

Carrie Boyer, *Investigation of Silver Doped Alumina Catalysts for the Aftertreatment of Diesel Exhaust*, Master's Thesis, Illinois State University, June 2003.

Paul Park, Christie Ragle, Carrie Boyer, "Steady-State Engine Testing of γ -alumina Catalysts under Plasma Assist for NO_x Control in Heavy Duty Diesel Exhaust," presented at Society of Automotive Engineers 2003 World Congress and Exhibition, Detroit, March 2003, SAE technical paper 2003-01-1186.

Carrie Boyer, Svetlana Zemskova, Paul Park, Lou Balmer-Millar, Dennis Endicott, Steve Faulkner, "Lean NO_x Catalysis Research and Development," presented at the Diesel Engine Emission Reduction Conference, Newport RI, August 24–28, 2003, to be published in the proceedings.

B. Development of Materials Analysis Tools for Studying NO_x Adsorber Catalysts

*Thomas Watkins, Larry Allard, Doug Blom, Michael Lance, Chaitanya Narula,
and Harry Meyer*

Oak Ridge National Laboratory

P.O. Box 2008, MS-6064

Oak Ridge, TN 37831-6064

(865) 574-2046; fax: (865) 574-4913; e-mail: watkinstr@ornl.gov

DOE Technology Development Area Specialist: Dr. Sidney Diamond

(202) 586-8032; fax: (202) 586-2476; e-mail: sid.diamond@ee.doe.gov

ORNL Technical Advisor: D. Ray Johnson

(865) 576-6832; fax: (865) 574-6098; e-mail: johnsondr@ornl.gov

Contractor: Oak Ridge National Laboratory, Oak Ridge, Tennessee

Prime Contract No: DE-AC05-00OR22725

CRADA with Caterpillar, CRADA No. ORNL02-0659

Objective

- Produce a quantitative understanding of the processing effects on nitrogen oxide (NO_x) adsorber catalyst technology that leads to an exhaust aftertreatment system with improved catalyst performance capable of meeting the 2007 emission requirements.

Approach

- Characterize engine-tested samples with X-ray diffraction (XRD), spectroscopy, and microscopy. Correlate findings with Cummins data and experience.

Accomplishments

- Established baseline characterizations of materials from various stages of the catalyst's life cycle.
- Verified the location and dispersion of the active elements within the washcoat of a catalyst.
- Determined the temperature dependence and thermal stability of adsorbed NO_x and SO_x species.

Future Direction

- Support continued characterization of new materials from various stages of the catalyst's life cycle.
 - Identify surface adsorbing species during nitration and sulfation via Raman spectroscopy.
 - Perform microstructural, microchemical, and crystallographic study of these new materials in simulated engine environments using an ex-situ reactor system with transmission electron microscopy (TEM) and HTK 900 stage with XRD.
-

Introduction

In order to meet the 2007 emission requirements for diesel exhaust, aftertreatment in diesel engines may be necessary. The technology necessary for 2007 will need to integrate aftertreatment with engine control systems. Currently, no commercial off-the-shelf technologies are available to meet these standards. Consequently, Cummins, Inc., is working to understand the basic science necessary to effectively utilize these catalyst systems. Oak Ridge National Laboratory (ORNL) is assisting with the materials characterization effort.

Base metal oxides (BMOs) are major components in current SO_x and NO_x adsorbers that Cummins seeks to use in NO_x adsorber catalyst systems. The function of these adsorbers is to collect oxy-sulfur (SO_x) and surface nitrite/nitrate (NO_x) species. These species are to be released from these surface sites during regeneration, where the adsorber BMO is either heated to some critical temperature or exposed to a reducing or reactant atmosphere. Sulfur poisoning of adsorber catalysts is a major problem that must be resolved for BMO-based emission reduction technologies to become commercially viable.

Approach

In general, the crystal structure, morphology, phase distribution, particle size, and surface species of catalytically active materials supplied by Cummins will be characterized using XRD, Raman spectroscopy, and electron microscopy. These materials will come from all stages of the catalyst's life cycle: raw materials, as-calcined, sulfated, regenerated, etc. Both ORNL and Cummins personnel have participated in this work.

Samples

A Cummins catalyst supplier provided core-drilled samples taken from cordierite

substrates containing the catalyst along the exhaust path for the following conditions: fresh (unused), degreened (zero desulfation hours), and engine-aged catalysts (>zero desulfation hours). Three main variables were considered with these samples: platinum (Pt) loading (1 or 2 wt %), substrate position (1, 2, 3, or 4 with 1 being the most upstream), and desulfation hours (the number of hours the catalyst system is at the desulfation temperature of $\sim 500^\circ\text{C}$; actual engine time is $\sim 150\%$ of desulfation time).

Results

X-ray

XRD was employed to aid in understanding the crystalline nature of the samples. As a fingerprint identifies a person, so does an XRD pattern identify a crystalline material. XRD data were collected using synchrotron radiation¹ for phase identification, crystallite size determination, and intensity comparisons. Three phases were observed in the engine-aged (desulfated) samples: platinum (Pt), the catalyst support, and cordierite ($\text{Mg}_2\text{Al}_2\text{Si}_5\text{O}_{18}$). Nominally, the intensities of the Pt peaks from the 2 wt % Pt samples were greater than those from the 1 wt % samples. In contrast, no Pt was observed in the fresh or degreened samples because of the fine dispersion of very small Pt particles (<1 nm) coupled with overlapping tails of peak from other phases.

The width of a peak² in an XRD pattern can be related to the crystallite size of the diffracting material. A crystallite is a region of coherent diffraction and can significantly contribute to peak broadening if it is smaller than $0.1 \mu\text{m}$. Typically, the crystallite size is much less than the grain size of a material as observed on the scanning electron microscope (SEM). In this context, crystallites can be thought of as sub-grains that are very small, perfect single crystals. This technique was particularly useful to monitor precious metal changes that occurred with catalyst aging. As the time at

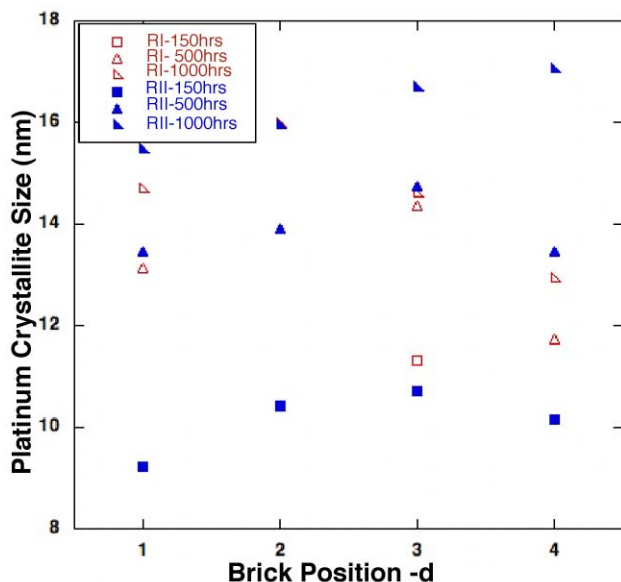


Figure 1. Platinum crystallite size as a function of catalyst substrate position. The red and blue symbols represent samples that contain 1 and 2 wt % Pt, respectively.

desulfation temperature ($\sim 500^{\circ}\text{C}$) increased, the Pt atoms began to sinter, forming larger crystallites. It was determined that the Pt crystallites were only losing defects, like dislocations, and were not adding or receiving new atoms of Pt.

Crystallite size as a function of brick position or distance from the engine is shown in Figure 1; also evident is the effect of desulfation hours. Brick position 1 is closest to the engine and is regarded as experiencing higher catalyst surface temperature as a result of the initial diesel light-off. Brick position 2, though, is regarded as having the highest bulk temperature. The 2 wt % Pt data show a moving Pt crystallite size maxima with brick position and desulfation hours, suggesting that the diesel light-off (or NO_x regeneration spike) was greatest at brick position 2 and seems to migrate downstream with desulfation time. This migration may be driven by Pt crystallite size. That is, heat from diesel light-off causes the Pt crystallite size to grow. When the crystallite size is approximately >14 nm, the light-off zone

occurs at downstream brick regions possessing smaller Pt crystallite sizes.

The crystallite sizes of the catalyst support increased with desulfation time at 500°C from 26 to 32 nm. These data, to some extent, co-relate with BET (the Brunauer-Emmett-Teller theory) surface area, although one should not overinterpret BET data because the absolute degree of change in the BET surface area is small. The BET surface area decreased from $10.5 \text{ m}^2/\text{g}$ in degreened samples to $7.3 \text{ m}^2/\text{g}$ in a 1000-h sample.

Spectroscopy

Three different spectroscopic techniques were used to characterize the adsorbed species: Raman spectroscopy, Fourier transform infrared spectroscopy (FTIR), and X-ray photoelectron spectroscopy (XPS). Raman spectroscopy measures the characteristic vibrational energy levels of molecules and crystals and so is very sensitive to any changes in bonding, stoichiometry and phase/symmetry. In this case, changes of the catalyst support vibrations with the length of desulfation time were monitored. The Raman peak width and position decreased and increased, respectively, as a result of the growth of the Pt particle size. These changes in the Raman spectra have been confirmed with XRD results and are believed to be caused by energy changes of the Pt valence orbital induced by Pt-support interaction. Although Raman spectroscopy could not directly measure the Pt particle size in these samples, the changes in the support Raman spectra with Pt size were calibrated for this specific catalyst formulation and so can be nondestructively used in the future for measuring Pt particle coarsening.

Raman spectroscopy is also very sensitive to adsorbed sulfur on the support. The vibration of the SO^{-2} species has a band at $\sim 960 \text{ cm}^{-1}$. Using a high-temperature stage that was not connected to an engine, the amount of sulfur present on a BaO support was monitored in situ in a reducing

atmosphere (see Figure 2). These preliminary spectra show the intensity of the band associated with SO_4^{12} decreasing in response to desulfation. Future work will focus on obtaining rates of desulfation, and thereby activation energies, for various compositions and after different periods of aging.

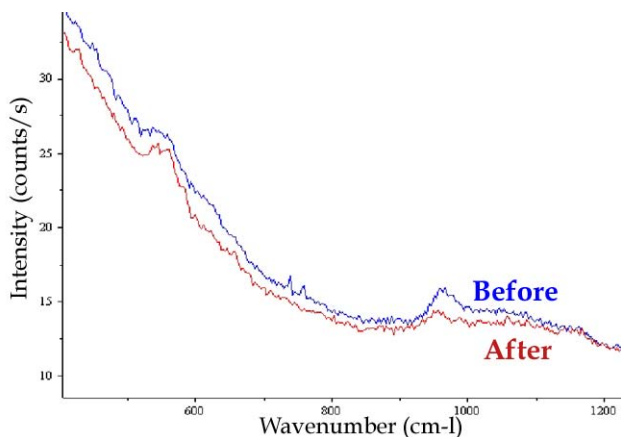


Figure 2. The Raman spectrum of a BaO support before and after desulfation. The intensity of Raman peak associated with SO_4^{-2} decreases.

FTIR also measures the vibrational energies of adsorbed species such as sulfates and carbonates, but it has a different level of sensitivity to these species from Raman spectroscopy. Here, FTIR spectra were collected only at room temperature. A degreased sample was first sulfated by exposure to 922 ppm SO_2/air at 400°C for 15 minutes. Then the sample was desulfated using 4% H_2 in N_2 at 500, 575 and 600°C to study the kinetics under idealized and controlled conditions. At 500°C , no desulfation had occurred; but $\sim 70\%$ of the sulfate was reduced at 575°C , and most of sulfate ($\sim 93\%$) was reduced at 600°C .

XPS identifies the presence and the chemical environment of atoms on a material surface (top 3.0 nm). In these experiments, determination of the presence and oxidation state of Pt on the surface was of interest. Only the fresh sample clearly showed a Pt 4f feature, which appears to be oxidized with a binding energy of ~ 72 eV versus ~ 71 eV for pure Pt metal. The Pt 4f

peaks in brick 1, with 500 desulfation hours and brick 3, with 1000 desulfation hours, were not confidently identified because of overlap of the Al 2p core level from the cordierite. For low-Pt loadings, it will be imperative to examine samples that are free from interference of the support/washcoat peaks. While differences were noted for the Pt core-level features from the fresh and engine-aged (desulfated) samples, it is not yet clear whether they are significant. Spot-to-spot variations on any single sample were often as large as sample-to-sample differences. One interesting observation is the presence of phosphorous in the sample taken from brick position 1, engine-aged for 500 desulfation hours with 1 wt % Pt loading. The presence of phosphorous was not observed in a sample from brick position 3, engine-aged for 1000 desulfation hours with 1 wt % Pt loading. Phosphorous is most likely to be deposited at the front end of the catalyst system (brick 1) because of engine lubricant blow-by.

Microscopy

TEM, scanning transmission electron microscopy (STEM), and electron probe microanalysis (EPMA) techniques were employed to characterize the microstructure of the NO_x trap catalysts. High-angle annular dark-field (ADF) images on the STEM provided a facile method for imaging the particles in high contrast and for measuring particle sizes (see Figure 3). These measurements were made on all observed samples (except the fresh specimen). Samples from the bricks with 1 wt % Pt loading with 150, 500, and 1000 desulfation hours displayed 8-nm, 9.5-nm, and 10.5-nm particles, respectively. These data are consistent with XRD analysis. It should be noted that the increase in the Pt particle size, although significant, is still comparable to that observed in commercial three-way catalysts for gasoline engines. The Pt particle size distribution in current commercial three-way catalysts for gasoline engines increases

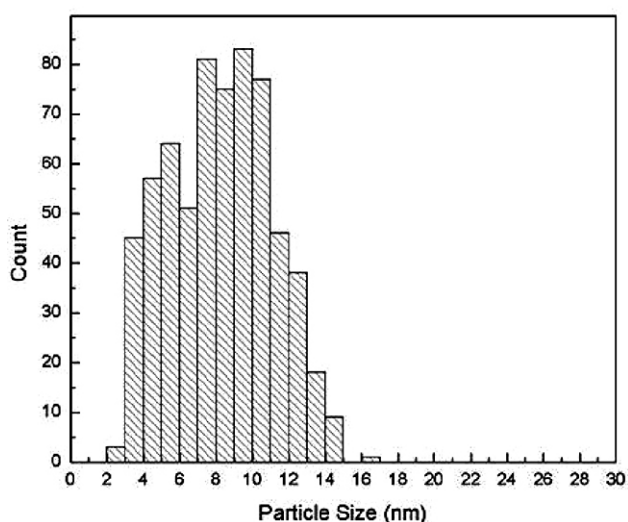
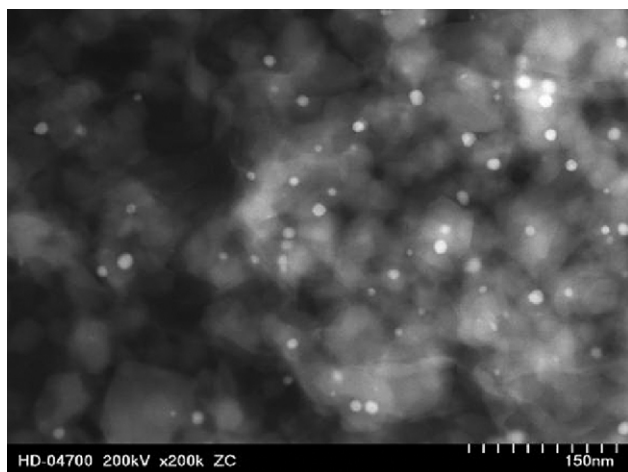


Figure 3. ADF image from the STEM showing Pt particles in bright contrast (top). The sample was from brick 2, loaded with 1 wt % Pt after 150 desulfation hours. Digital processing yields distribution of Pt particles, with statistics as shown (bottom). The mean, median, and standard deviation for 648 Pt particles were 8.2, 8.3 and 2.8 nm, respectively.

from being centered at 1.3 nm to being centered at 5.7 nm after 50,000 miles of operation.

EPMA was used to determine the bulk distributions and quantitative measurements of the Pt and sulfur species by acquiring X-ray counts from small regions from the outer surface of the washcoat layer into the cordierite framework. These measurements mapped Pt at the 1 wt % level and sulfur (1

wt % Pt, 500 and 1000 desulfation hours), which varied by position (inhomogeneously distributed). Backscattered electron images of the cross-section of the catalyst brick framework and washcoat layers were compared to X-ray distribution maps of the various elemental components. Platinum showed concentrations primarily at free surfaces within and external to the two washcoat layers. Typically, a higher concentration of Pt was observed near free surfaces such as drying cracks, pores, and the interface between the inner and outer washcoats (see Figure 4). Pt did not appear to change in general concentration with aging, even though particle sizes increased significantly.

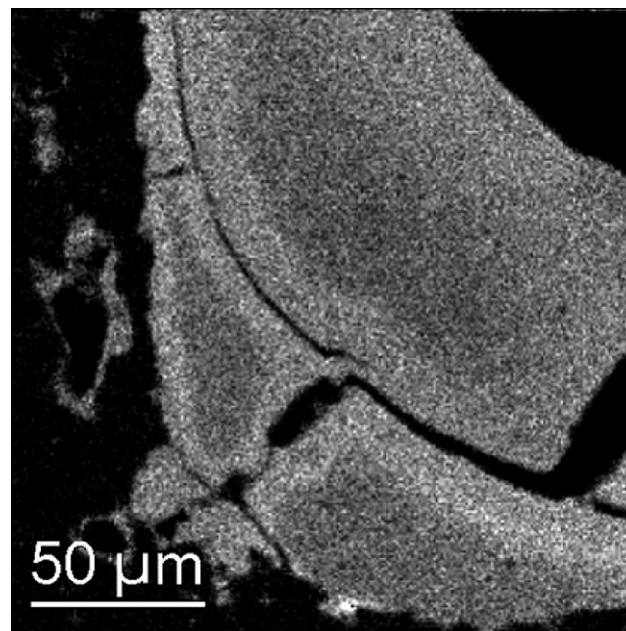


Figure 4. Platinum X-ray map in the sample from catalyst substrate position 2, loaded with 1 wt % Pt after 500 desulfation hours. Note concentration of Pt at free surfaces in washcoat. This concentration remained essentially constant with aging treatments.

Summary

All techniques (XRD, microscopy, and spectroscopy) have proved to be very useful in monitoring Pt changes in size and location in these catalytic samples. The

observed increase in the Pt particle size, although significant, is still comparable to that observed in commercial three-way catalysts for gasoline engines. Although Raman spectroscopy could not directly measure the Pt particle size in these samples, the changes in the catalyst support spectra along with changes in Pt size were calibrated for this specific catalyst formulation and were used for measuring Pt particle coarsening. The Raman and XPS techniques show promise for future in-situ desulfation work and chemical state identification of surface species, respectively.

References

1. A. Habenschuss, G. E. Ice, C. J. Sparks, and R. A. Neiser, "The ORNL Beamline at the

National Synchrotron Light Source," *Nuc. Instr. and Meth.* A266 215-9 (1988).

2. B. D. Cullity, *Elements of X-Ray Diffraction*, 2nd ed., Addison-Wesley, Reading MA, 1978, A, p.87, and B, pp. 101-2.

Publications/Presentations

J. Parks, A. Watson, B. Epling, L. Campbell, R. England, N. Currier, A. Yezerets, H. Fang, T. Yonushonis, T. Gallant, T. Watkins, D. Blom, L. Allard, M. Lance, H. Meyer, and C. Narula, "NO_x Adsorber Catalyst Durability: Light- and Heavy-Duty Perspective," presented by J. Parks at the 9th Diesel Engine Emissions Reduction (DEER) Conference, Newport, Rhode Island, August 28, 2003.

C. Development of NO_x Sensors for Heavy Vehicle Applications

Timothy R. Armstrong, Fred C. Montgomery, David L. West, J. Visser, and R. Soltis**

Oak Ridge National Laboratory

P.O. Box 2008, MS-6084

Oak Ridge, TN 37831-6084

(865) 574-7996; fax: (865) 574-4357; e-mail: armstrongt@ornl.gov

**Scientific Research Laboratory, Ford Motor Company*

DOE Technology Development Area Specialist: Dr. Sidney Diamond

(202) 586-8032; fax: (202) 586-2476; e-mail: sid.diamond@ee.doe.gov

ORNL Technical Advisor: D. Ray Johnson

(865) 576-6832; fax: (865) 574-6098; e-mail: johnsondr@ornl.gov

Contractor: Oak Ridge National Laboratory, Oak Ridge, Tennessee

Prime Contract No: DE-AC05-00OR22725

CRADA No. ORNL01-0627with Ford Motor Company

Objectives

- Develop a nitrogen oxides (NO_x) sensor, to be used in systems for on-board remediation of diesel engine exhaust, that has an operating temperature of 600–700°C and can measure NO_x concentrations from 0 to 1500 ppm at oxygen levels from 5 to 20 vol %.

Approach

- Fabricate prototype sensing elements by patterning electronically conductive and catalytic layers onto oxygen-ion conducting substrates. The sensing elements are characterized for NO_x response, oxygen sensitivity, and response time.
- Analyze the results, along with microstructural characterization, to determine the correct combination of materials chemistry, materials processing, and sensor design required for the desired sensor performance.

Accomplishments

- Completed an automated test stand that can characterize sensor performance at temperatures up to 900°C.
- Examined more than 30 different materials combinations for “mixed-potential” sensing and identified commonalities among the responses.
- Showed that the two main barriers to application of the mixed-potential approach are the differing response to NO and NO₂ and oxygen sensitivity.
- Showed that external applied electrical signals (“bias”) enhance sensing performance.

Future Direction

- Focus future work in sensing materials and sensor geometry on investigating cross-sensitivity (to CO, hydrocarbons, and H₂O), optimizing sensor response time, and addressing the difficulties with the mixed-potential approach.
 - Concentrate sensor design efforts on fabricating working prototype sensors and evaluating their long-term stability and performance in vehicle exhaust.
-

Introduction

The three main pollutants in combustion exhausts from low-sulfur fuels are carbon monoxide (CO), hydrocarbons (HC), and NO_x (a mixture of NO and NO₂). Currently, for fuel-injected passenger cars, a three-way catalyst (TWC) is employed that greatly reduces the levels of all three pollutants. The TWC is effective only within a narrow range of oxygen (O₂) concentrations in the exhaust, losing its effectiveness for NO_x removal at higher O₂ contents. Therefore the TWC cannot be employed for NO_x remediation of exhausts from diesel and lean-burn gasoline engines, as these tend to be O₂ rich.

These exhausts will require on-board NO_x remediation with techniques such as selective catalytic reduction (SCR) with reagent (HC and/or urea) injection. The amount of reagent injection during SCR is critical, as enough must be supplied to completely decompose the NO_x, but the addition of excess must be avoided. Therefore it is essential to develop sensors that can rapidly and accurately assess the NO_x levels in these exhausts and enable improved emissions control and on-board diagnostics.

In this research, we are developing NO_x sensors that can be used in diesel and lean-burn engine exhausts. Initial efforts were focused on developing sensing elements operative at 600–700°C, capable of measuring up to 1500 ppm NO_x and capable of operating in 5–20 vol % O₂. This project is a cooperative research and development effort with Ford Motor Company, in which Ford will collaboratively test materials and sensors developed by ORNL.

Approach

The approach in general is to fabricate and characterize sensing elements (as opposed to working sensors). One geometry selected for prototype sensing elements is shown in Figure 1. This element consists of screen-printed conductive [reference electrode (RE) and current collector (CC)] layers and catalytic [sensing electrode (SE)] layers on a yttria-stabilized zirconia (YSZ) substrate. The YSZ substrates are fabricated in-house from commercially obtained YSZ powder by tape-casting, lamination, and sintering at 1350°C. Inks for screen-printing the conductive and catalytic layers are also fabricated in-house, using proprietary materials and methods. The screen-printed layers are normally fired onto the sintered substrate at lower temperatures (900–1100°C) than those used to sinter the substrate.

The sensing element shown in Figure 1 is designed for use as a mixed-potential sensor,¹ and the voltage between the RE and CC is used as a sensing signal. A voltage develops upon exposure to NO_x as a result of the differing electro-chemical behavior of the RE and the SE/CC combination.

We are also exploring sensing elements that require the use of external electrical signals (biasing) to measure NO_x. The geometry of these elements usually differs from that shown in Figure 1, and, in this instance, the electrical resistance of the sensing element is used to measure the NO_x concentration.

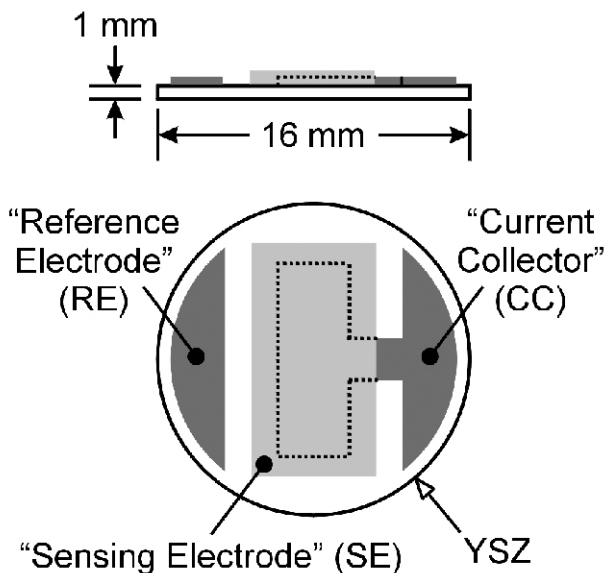


Figure 1. Schematic of specimen geometry for a mixed-potential sensing element.

Prototype sensing elements are evaluated both microstructurally and for sensing performance. Sensing performance is characterized by recording the sensing signal (voltage or resistance) when it is exposed to varying concentrations of NO_x at a fixed O_2 level or varying O_2 levels at fixed concentrations of NO_x . As mentioned previously, “ NO_x ” is a mixture of nitrogen oxides (primarily NO and NO_2), with NO being the dominant species at high temperatures (above 600°C). Typically, in our characterization, we expose the sensing element to either NO or NO_2 .

Results

Figure 2 shows a plan view of a chromite family SE of a sensing element fabricated with the geometry shown in Figure 1. The chromite SE features a relatively open and porous microstructure. This porous microstructure, obtained by screen-printing a dispersion of the chromite and sintering at 1100°C , should enhance the sensing performance.

Figure 3 shows a trace of the measured voltage from a mixed-potential sensing element as the input NO_2 level was varied at

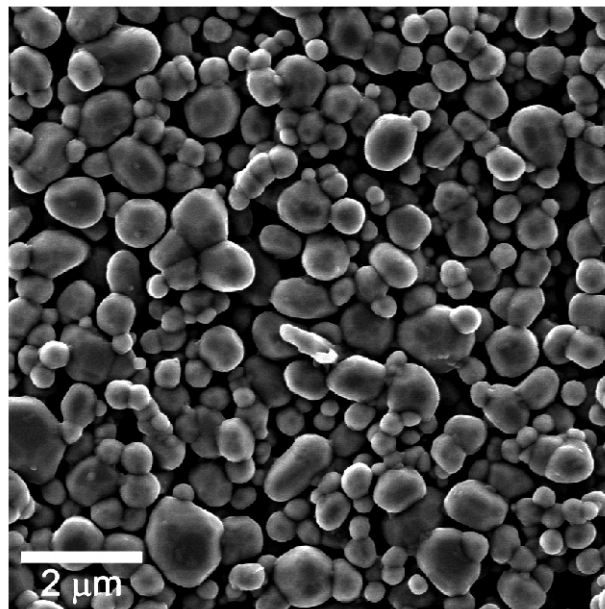


Figure 2. Microstructure of a chromite sensing electrode.

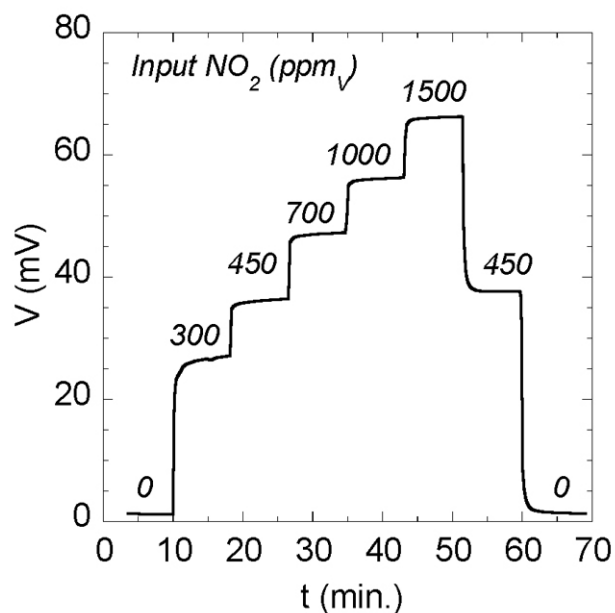


Figure 3. Response trace of a mixed-potential sensing element as the input NO_2 is varied at 700°C in 7 vol % O_2 .

constant O_2 (7 vol %) at a testing temperature of 700°C . This sensing element, constructed using platinum (Pt) as the RE and CC material, and $\text{La}_{0.6}\text{Sr}_{0.4}\text{Co}_{0.8}\text{Fe}_{0.2}\text{O}_3$ (LSCF) as the SE material, gives a strong and reproducible response to NO_2 at temperatures

in the range of 600 to 700°C. We have evaluated some 30 different oxides as SE materials; the criteria for selection usually are either literature reports of interesting electrochemical or catalytic behavior, or prediction of such behavior based on crystallo-chemical considerations. Many of the materials have been obtained from commercial sources, but in-house synthesis using combustion synthesis has also been employed. Virtually all the materials have exhibited the logarithmic response to NO₂ shown in Figure 4, which shows the NO₂ response curves for sensing elements using LSCF and the ferrite material NiCr₂O₄ as the SE material. Platinum was used as the RE and CC material (Figure 1) for both of the sensing elements of Figure 4.

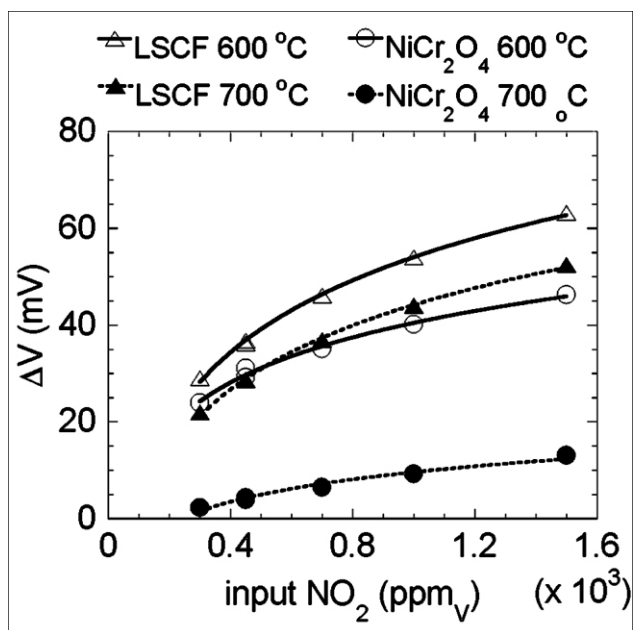


Figure 4. NO₂ response curves (in 7 vol % O₂) for sensing elements with LSCF and NiCr₂O₄ sensing electrodes.

Currently we are working to eliminate the two main weaknesses of these mixed-potential sensing elements. The first difficulty with them is illustrated in Figure 5. In it is plotted the sensor response for the same two elements as in Figure 4, except that the O₂ concentration has been varied at constant input NO₂. The sensor response

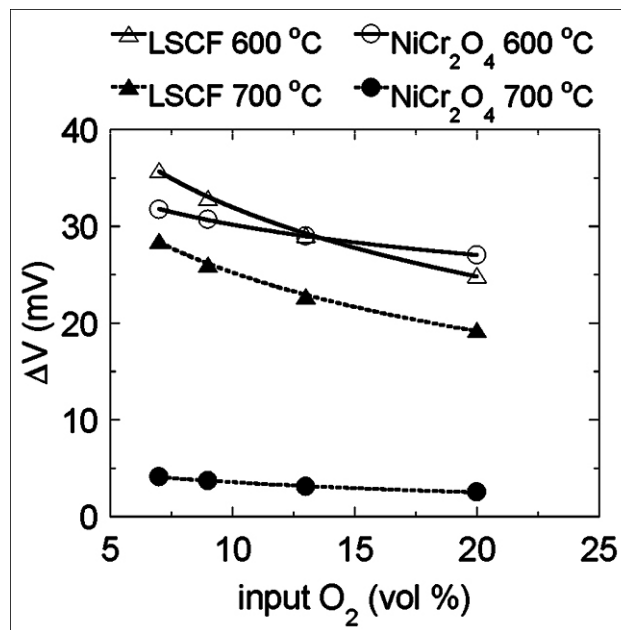


Figure 5. O₂ sensitivity (at 450 ppm input NO₂) of sensing elements with LSCF and NiCr₂O₄ sensing electrodes.

varies logarithmically with input O₂, which means that use of these sensing elements would require a simultaneous, independent measure of the O₂ concentration, or the portion of the exhaust gas used for sensing would have to be pre-treated to fix the O₂ concentrations.

The second difficulty with these mixed-potential sensors is illustrated in Figure 6, which shows the measured output of a sensing element subjected to 5-minute pulses of either NO₂ or NO during a heating and cooling cycle. It can be seen that the response to NO is weaker and of opposite sign to that to NO₂, irrespective of the temperature. The differing sign is believed to arise from the fact that the sensing reaction for NO involves NO being oxidized to NO₂, whereas the sensing reaction for NO₂ involves NO₂ being reduced to NO (ref. 2). The differing signs of the response to NO and NO₂ have important ramifications for sensor design if a mixed-potential sensing element is to be employed. The NO/NO₂ ratio in the exhaust gas would have to be known, or means would have to be taken to convert the

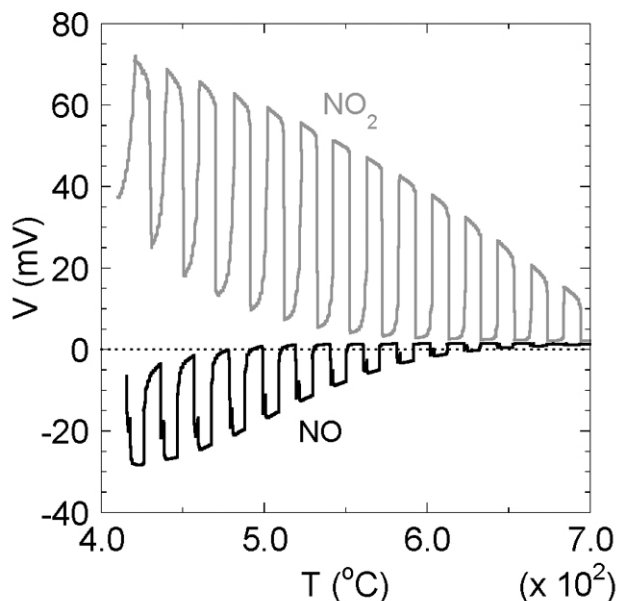


Figure 6. Sensing element response to input NO and NO₂ as a function of temperature. Data collected while heating and cooling at 5°C/min in 7 vol % O₂.

NO_x to near 100% NO₂ (or NO) in the portion of the exhaust gas used for sensing.

The difficulties mentioned have been addressed somewhat by the application of external electrical signals or biasing. In this approach, a dc electrical signal is applied to a sensing element of different geometry from that shown in Figure 1, and the resistance (R) is monitored. This is similar to techniques that have been employed for “semiconductor gas sensors.”³

Figure 7 shows the changes in resistance of a sensing element due to the indicated concentrations of NO and NO₂ at 700°C in 7 vol % O₂. For the data shown there, a constant current (I) was imposed across the sample and the dc voltage (V) was measured. The changes in resistance were then computed from

$$\Delta R^{x \text{ ppm NO}_x} = (\Delta V^{x \text{ ppm NO}_x}) / (I),$$

where $\Delta V^{x \text{ ppm NO}_x} = V^{x \text{ ppm NO}_x} - V^{0 \text{ ppm NO}_x}$.

Comparing Figure 7 with Figure 6, the response to NO and NO₂ is now of the same

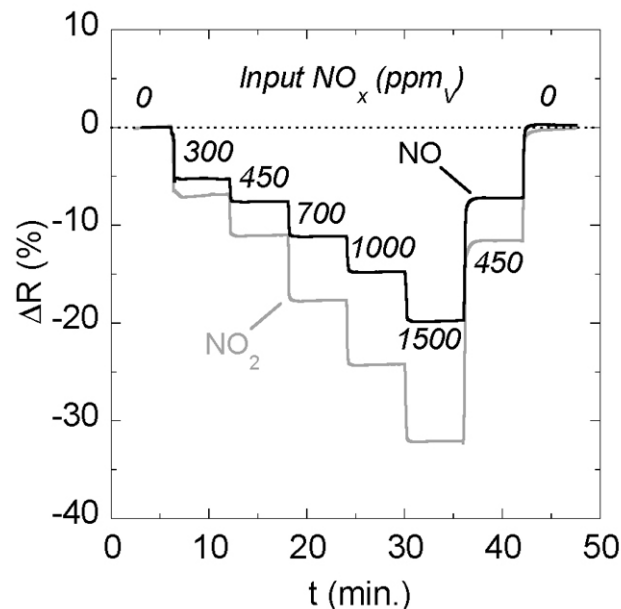


Figure 7. Computed resistance (R) trace in NO and NO₂ for a current-biased sensing element operating at 700°C in 7 vol % O₂.

algebraic sign and nearly the same magnitude. If, through the proper combination of sensing element design and materials selection, the responses to NO and NO₂ could be equalized, the sensing element would be a total NO_x sensor, and the need to either know the NO/NO₂ ratio or convert the NO_x prior to sensing would be eliminated.

The biasing approach also appears to offer some hope of ameliorating the O₂ sensitivity. Figure 8 shows that with a voltage-biased sensing element, operated at 600°C, the oxygen sensitivity (at 450 and 1500 ppm input NO) could be largely eliminated. This would eliminate the need in a working sensor to independently measure, or fix at a pre-determined concentration, the O₂ level in the portion of the exhaust gas used for sensing.

Conclusions

An automated test stand for evaluating NO_x sensing elements has been completed. Specimen geometries for evaluating mixed-potential sensing elements have been

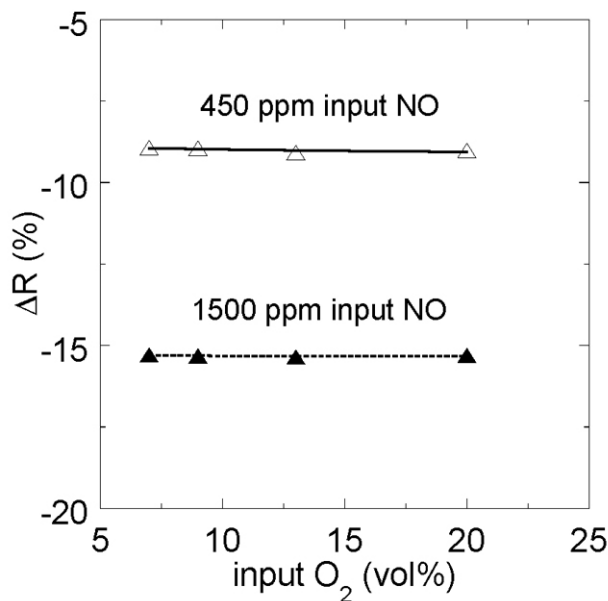


Figure 8. Resistance (R) change as a function of O₂ level for a voltage-biased sensing element operating at 600°C.

determined. The testing results to date indicate that these elements perform well with regard to sensing NO₂, but the response to NO is weaker and opposite in sign. Sensitivity to O₂ also appears to be a difficulty. Use of externally applied electrical signals has shown promise for addressing these difficulties.

Future work on sensing element materials and geometry will be aimed at addressing four main issues: NO sensitivity/selectivity, O₂ sensitivity, cross-sensitivity to potentially interfering gases (H₂O, CO, and hydrocarbons), and response time. Future work on sensor design is envisioned to focus on issues of long-term stability and optimization for use in vehicle exhaust streams.

References

1. N. Miura, G. Lu, and N. Yamazoe, "Progress in Mixed-Potential Type Devices Based on Solid Electrolyte for Sensing Redox Gases," *Solid State Ionics*, 136–137, 533–42, (2000).
2. W. Gopel, R. Gotz, and M. Rosch, "Trends in the Development of Solid State Amperometric and Potentiometric High Temperature Sensors," *Solid State Ionics*, 136–137, 519–31 (2000).
3. K. Ihokura and J. Watson, *The Stannic Oxide Gas Sensor*, CRC Press, Boca Raton, FL, 1994.

D. Ultra-High-Resolution Electron Microscopy for Characterization of Catalyst Microstructures and Deactivation Mechanisms

*L. F. Allard, D. A. Blom, K. K. Lester, C. K. Narula, and M. A. O'Keefe**

Oak Ridge National Laboratory

P. O. Box 2008, MS-6064

Oak Ridge, TN 37831-6064

(865) 574-4981; fax: (865) 576-5413; e-mail: allardlfjr@ornl.gov

**Department of Materials Science and Engineering, Lawrence Berkeley National Laboratory, Berkeley, CA*

DOE Technology Development Area Specialist: Dr. Sidney Diamond

(202) 586-8032; fax: (202) 586-2476; e-mail: sid.diamond@ee.doe.gov

ORNL Technical Advisor: D. Ray Johnson

(865) 576-6832; fax: (865) 574-6098; e-mail: johnsondr@ornl.gov

Contractor: Oak Ridge National Laboratory, Oak Ridge, Tennessee

Prime Contract No: DE-AC05-00OR22725

Objectives

- Develop and utilize the new capabilities and techniques of ultra-high resolution transmission electron microscopy (TEM) to characterize the microstructures of catalytic materials that are of interest for reduction of NO_x emissions in diesel and automotive exhaust systems.
- Relate the effects of reaction conditions on the changes in morphology of heavy metal species on "real" catalyst support materials (typically oxides).

Approach

- Use new field-emission microscopes at the High Temperature Materials Laboratory (HTML) at Oak Ridge National Laboratory (ORNL), designed for imaging of catalyst particles at near-atomic level, to develop techniques applicable for imaging catalysts at sub-Ångstrom levels with the new Aberration-Corrected Electron Microscope (ACEM).
- Conduct studies of microstructural changes in locally synthesized model NO_x trap catalyst samples treated both in static bench reactors and in a special ex-situ catalyst reactor system especially constructed to allow appropriate control of the reaction.

Accomplishments

- Obtained the first results of microstructural studies of a series of model NO_x trap catalyst materials comprising platinum (Pt) on mixed oxides. The materials were synthesized in the new catalyst synthesis facility within the HTML.
- Collaborated successfully with Lawrence Berkeley National Laboratory (LBNL) colleagues to demonstrate a new capability for high-resolution imaging using the thru-focal series (TFS) reconstruction technique to allow determination of nanoparticle structure and shapes at the atomic level.

Future Direction

- Use new high-resolution electron microscopy imaging techniques, along with energy-dispersive X-ray microanalysis, on the 2010F FE-TEM (and other HTML instruments) to characterize systematic series of model NO_x trap catalyst materials in order to relate reaction conditions in both bench-top and ex-situ reactors to changes in microstructure.
- Successfully initiate a TFS reconstruction capability at the HTML on JEOL 2010F FE-TEM and correlate this imaging technique to annular dark-field (ADF) scanning TEM (STEM) images of fine particles.

Introduction

Development of New Model NO_x Trap Catalysts

We have synthesized a model NO_x trap catalyst composed of 2 wt % Pt on a mixed CeO₂-ZrO₂-La₂O₃-BaO-Al₂O₃ support material (or, more formally, 2% Pt-98% [10%CeO₂-ZrO₂-90% (2%La₂O₃-98%BaO.6Al₂O₃)]). This model system has been shown to retain its beneficial surface properties even after thermal aging at 1050°C. We have begun studying the thermal durability/stability and catalyst restructuring behavior under exposure to diesel and gasoline lean and rich simulated exhaust. The material was prepared as follows:

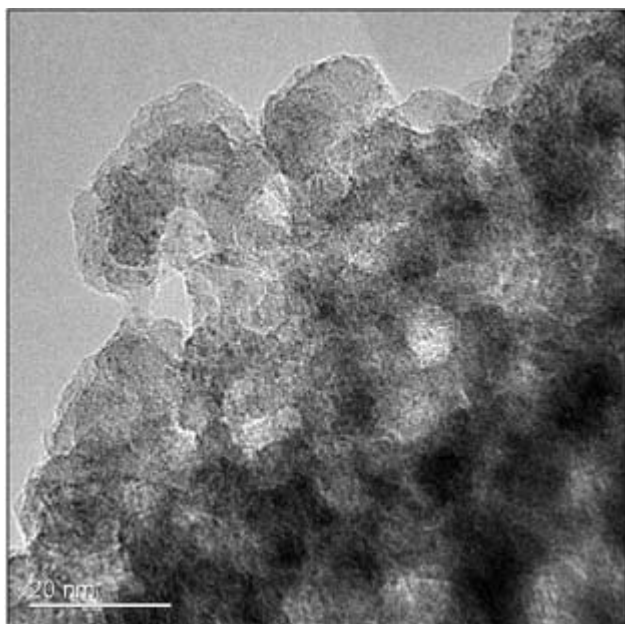
1. Impregnation of Ba(NO₃)₂ on commercial high-surface-area alumina, followed by pyrolysis and by sintering at 500°C.
2. Impregnation of step 1 material with lanthanum nitrate, then pyrolysis, and sintering at 750°C.
3. Ball milling step 2 material with commercial high-surface-area CeO₂-ZrO₂. Impregnation of step 3 material with H₂PtCl₆ · H₂O, pyrolysis, and calcination at 500°C to produce the final “fresh” or as-prepared catalyst material.

Both fresh and thermally aged materials have been characterized to a significant extent to date, as this information is needed to establish a baseline of behavior prior to exposures under simulated exhaust conditions. Fresh samples were prepared by

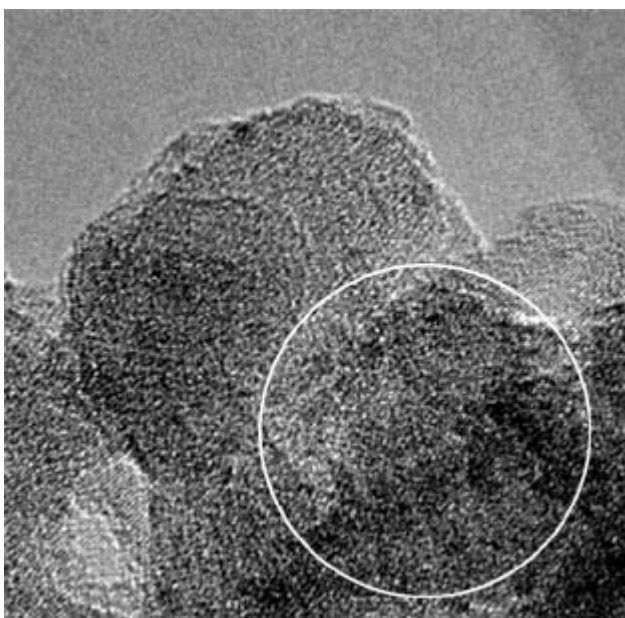
impregnation of Pt on both hand-milled and ball-milled powders; the hand-milled specimens were made with very small quantities of the individual powders and showed the large, discrete aggregates of each constituent. A successful dispersion of Pt clusters was achieved on this sample, with uniform clusters 0.5–1.5 nm in size visible on most powder support aggregates. The ball-milled samples were made using a larger quantity of constituent powders so that 70 g finally was synthesized. Some typical results on the Pt particle distributions on these samples and the effects of additional thermal aging are given in the following paragraphs (ball-milled specimens).

Fresh samples

The powder support materials in the ball-milled fresh sample retained their discrete nature, but aggregates were clearly much smaller and more interspersed than in the hand-milled sample. Figure 1a is a bright-field TEM image from the JEOL 2010F that apparently shows a uniform distribution of clusters (“measles”) on the surface of the alumina phase. At higher magnification (Figure 1b), however, the lattice structure of the alumina becomes increasingly visible, leading to ambiguity in the capability to precisely identify and quantify the sizes and morphology of the clusters. ADF imaging using the Hitachi dedicated STEM shows the Pt clusters in bright contrast (Figure 2), albeit at lower resolution than the bright-field images taken using the 2010F. Energy-



(a)



(b)

Figure 1. (a) Bright-field TEM image of Pt clusters on alumina phase in fresh BaAlCeZrLa NO_x trap catalyst. Pt particles look like “measles” on surface. (b) High-resolution image of area in 1a, showing difficulty in ability to determine exact location and size of Pt clusters. EDS data taken from circled area.

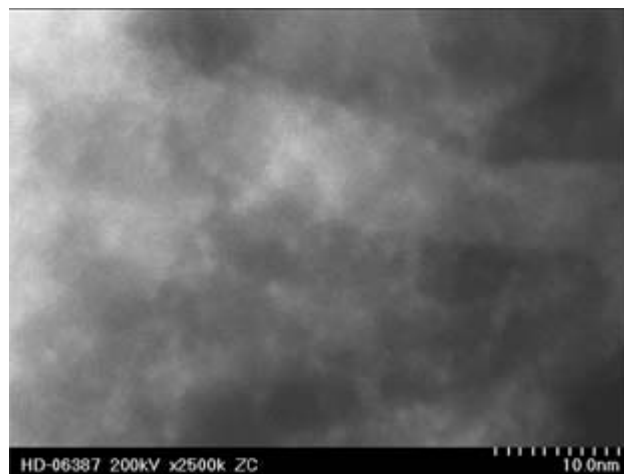


Figure 2. ADF STEM image showing Pt clusters distributed over the surface of alumina phase in fresh NO_x trap catalyst.

dispersive spectroscopy (EDS) spectra from small areas in both Figures 1b and 2 showed the presence of Pt, confirming that the support did indeed contain Pt. The EDS spectrum in Figure 3 was acquired, for example, from the circled region of Figure 1b. The contrast in both microscopes suggests that the Pt clusters on the fresh ball-milled sample were two-dimensional “rafts” of atoms, rather than discrete, three-dimensional crystals. The capability to describe accurately the precise morphology of such clusters will require the highest-resolution imaging provided by aberration-corrected STEM and TEM techniques.

The barium oxide (baria) phase in the ball-milled sample is shown in Figure 4. This phase was clearly crystalline, while baria typically forms as an amorphous phase. EDS showed carbon in the spectrum; as it is known that BaO is unstable in the presence of CO₂, it is likely that the baria phase transformed to barium carbonate. It is difficult to tell by TEM whether the fine-grained crystalline structure seen in Figure 4a is present through the entire volume of the particle or is essentially a crystalline surface coating with an amorphous baria interior. These results are consistent with X-ray diffraction studies of barium-oxide-based

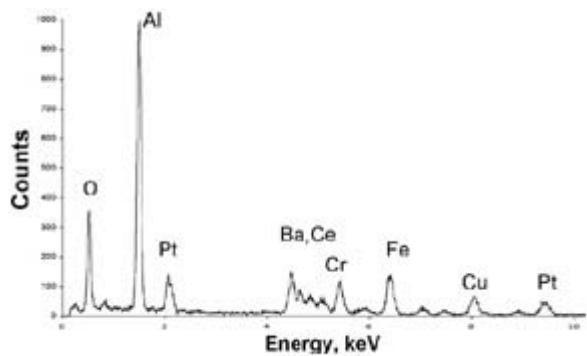


Figure 3. EDS spectrum showing Pt in area circled in Fig. 1b. Peaks of Cr, Fe and Cu are artifacts from specimen holder.

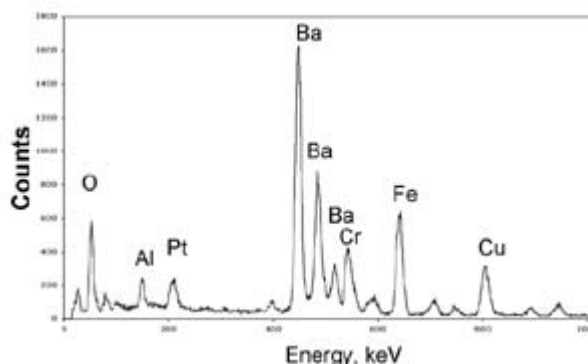
NO_x trap materials where barium carbonate peaks are seen. The Pt clusters on this sample were not readily visible in the TEM image, but EDS (Figure 4b) from the area of the barium carbonate particle in Figure 4a showed Pt similar to the Pt seen on the alumina phase. ADF STEM images also showed Pt clusters similar to those seen on the alumina. The small aluminum peak seen in this spectrum arises from adjacent alumina aggregates and is not consistent with the barium-rich phase's being a barium aluminate.

Effects of thermal aging

To get an initial baseline indication of the morphological changes in the fresh sample as a result of additional thermal aging, a small quantity of the powder was aged at 500°C in air for 4 hours and then reexamined in the TEM. Figures 5a and 5b are ADF images showing the large effects on catalyst morphology that resulted. The nominal 1-nm Pt clusters grew into discrete particles on the order of 20–40 nm in size. The barium carbonate phase grew into acicular crystals. As before, EDS results were

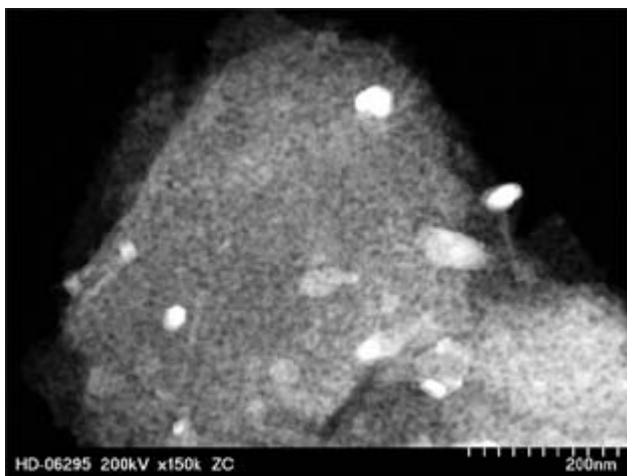


(a)

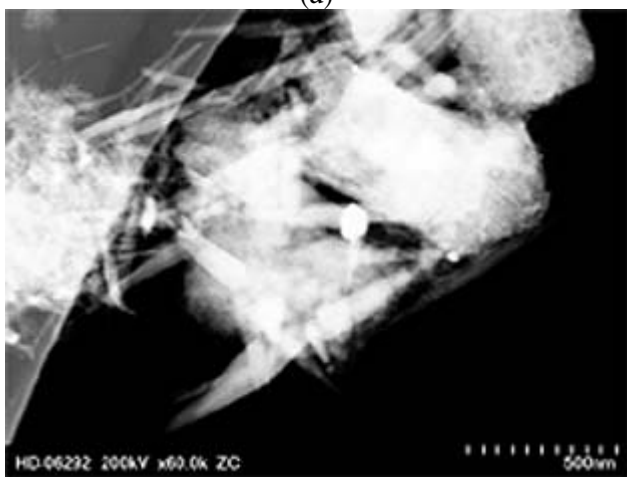


(b)

Figure 4. (a) Area of catalyst containing primarily baria. No specific signs of Pt cluster distribution are evident in this image. Polycrystalline structure seen in this lattice image consistent with amorphous baria recrystallizing to form barium carbonate. (b) EDS spectrum from area in Fig. 4a, showing presence of Pt on barium carbonate support, even though no Pt clusters are evident.



(a)



(b)

Figure 5. (a) ADF image of alumina support aggregate in NO_x trap catalyst after thermal aging. Large bright particles are Pt; note strong faceting (arrowed). (b) ADF image of another area in thermally aged catalyst, showing needles of barium carbonate and faceted Pt particles.

consistent with barium carbonate rather than a barium aluminate phase. No significant change was noted in the alumina, ceria, or zirconia phases.

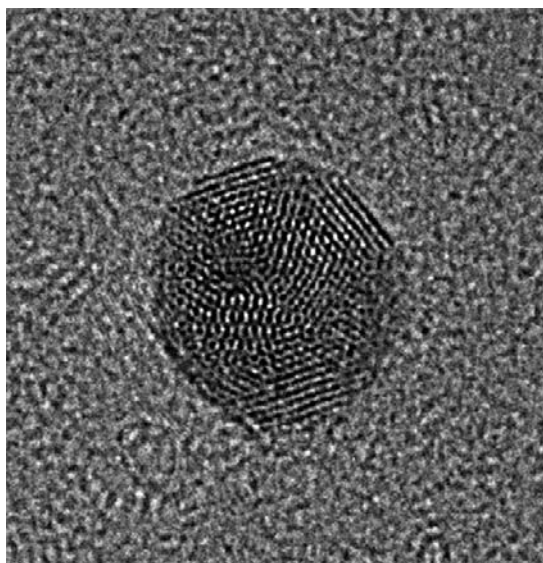
Results of studies of controlled reactions in simulated exhaust compositions in both the ex-situ TEM reactor and a bench-top flow reactor will be reported in a quarterly report.

Development of Imaging Techniques for Characterization of Nanoparticle Structure and Morphology

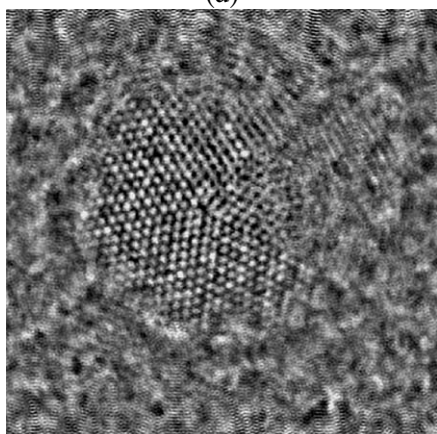
ORNL has undertaken a collaboration with LBNL to use new high-resolution imaging techniques for characterization of the structure and morphology of nanoparticles such as heavy metal species that are important in all catalytic materials, including the NO_x trap materials. These techniques involve special image acquisition and processing methods for bright-field TEM images, which will allow us to achieve a resolution near the 1-Å level in the ACEM. The method is called TFS reconstruction and will complement the ACEM's projected ability to generate sub-Ångstrom images using dark-field STEM methods. The advantage in characterization of the actual structure of a nanoparticle provided by this advanced imaging capability, and some of the early test results on heterogenous systems, are shown in Figure 6. Figure 6a is an image of a 7-nm-diameter particle of gold, taken on a field-emission TEM at LBNL at the best bright-field image resolution of about 1.8 Å. With TFS reconstruction, a processed image at a resolution of about 1 Å can be generated, as shown in Figure 6b. This figure shows the "multiple twin" structure of the gold particle that is not evident in the original image. Such images will provide a better opportunity to determine exactly which crystal planes are exposed at the particle surface, which is important in determining the mechanisms of catalytic reactions. We plan to subject selected NO_x trap materials to similar characterization.

Conclusions

The work on development of a capability to synthesize in-house experimental model NO_x trap catalysts has been initiated. We have a new model NO_x trap system that will be our baseline NO_x trap for studies to



(a)



(b)

Figure 6. (a) Bright-field TEM image of 70-nm gold particle, taken at optimum focus with resolution of 1.8 Å. Atom columns are “black.” (b) Image of same gold particle, after TFS processing, showing “white” atom columns at 1 Å resolution. The multiple twinning structure is seen that was not evident in the original image.

improve materials for diesel exhaust emission control. The work on imaging of catalysts using advanced image processing techniques to achieve ultra-high resolution in bright-field images will complement the sub-Ångstrom imaging capabilities expected with the ACEM.

Acknowledgements

Figure 1a was used courtesy of S. J. Pennycook of ORNL. High-resolution images of the gold particle in Figure 6 were recorded at the National Center for Electron Microscopy at LBNL.

Publications

M. A. O’Keefe, E. C. Nelson, and L. F. Allard, “Focal-Series Reconstruction of Nanoparticle Exit-Surface Electron Wave,” *Microscopy and Microanalysis 2003*.

E. Microstructural Changes in NO_x Trap Materials under Lean and Rich Conditions at High Temperatures

C. K. Narula, K. Lester, and L. F. Allard

Oak Ridge National Laboratory

P.O. Box 2008, MS 6066

Oak Ridge, TN 37831-6066

(865) 574-8445; fax (865) 574-6098; e-mail: narulack@ornl.gov

C. Goralski, J. Li, J. Theis

Ford Research Laboratory, MD 3179

2101 Village Road

Dearborn, MI 48124

(313) 248-5576; fax (313) 594-2963; e-mail: cgoralsk@ford.com

DOE Technology Development Area Specialist: Dr. Sidney Diamond

(202) 586-8032; fax: (202) 586-2476; e-mail: sid.diamond@ee.doe.gov

ORNL Technical Advisor: D. Ray Johnson

(865) 576-6932; fax: (865) 574-6098; e-mail: johnsondr@ornl.gov

Contractor: Oak Ridge National Laboratory, Oak Ridge, Tennessee

Prime Contract No: DE-AC05-00OR22725

Objective

- Facilitate deployment of a NO_x trap for lean diesel or gasoline exhaust by
 - investigating materials issues related to deterioration of performance in NO_x traps upon aging as a result of thermal and sulfation-desulfation cycles
 - investigating materials that are robust under the lean NO_x trap operating conditions

Accomplishments

- Determined the microstructural changes that occurred in a supplied lean NO_x trap system (based on Pt/BaO-Al₂O₃ and CeO₂-ZrO₂ materials) upon aging on a pulsator at Ford Motor Company
 - Lean and rich aged samples showed that the sintering of platinum (Pt) particles occurs during aging, and barium (Ba) migrates into the ceria-zirconia layer. Both of these factors reduce the Pt-Ba oxide surface area where NO_x adsorption and reduction take place during lean and rich cycles, respectively.
 - The stoichiometric aging also leads to the migration of Ba into the ceria-zirconia layer, but the sintering of Pt is less severe.
- Synthesized model materials Pt/BaO.6Al₂O₃ and [10%CeO₂-ZrO₂-90%(2%La₂O₃-98%BaO.6Al₂O₃)]. The latter is a better representative of this class of NO_x trap systems.
 - The microstructural evaluation of freshly prepared materials by X-ray diffraction (XRD) and transmission electron microscopy (TEM) shows the formation of some Ba aluminate.

- The study of microstructural changes on aging under different operating conditions is in progress.
- Updated the ex-situ reactor and enhanced its capabilities to enable treatment of TEM samples under lean, rich, or stoichiometric conditions. This reactor is capable of rapid screening of the model catalyst powders for their durability in exhaust under lean or rich operating conditions for diesel and gasoline engines.
- Equipped the synthesis laboratory to enable preparation of NO_x trap materials. Several items are on order for setting up a bench-top flow reactor in a laboratory at the National Transportation Research Center (NTRC).

Future Direction

- Evaluate model catalyst systems on a bench-top flow reactor for their efficiency and durability as NO_x traps under simulated diesel and gasoline conditions (with or without SO_x in the simulated exhaust). These results will provide a benchmark for evaluation of new materials.
- Conduct the microstructural characterization of model NO_x trap powders after aging under lean, rich, or stoichiometric conditions on a bench-top flow reactor and characterize TEM samples on the ex-situ microreactor.
- Investigate new materials that can withstand NO_x trap operating conditions without detrimental structural changes.

Introduction

NO_x traps are at the forefront of various strategies under investigation to treat NO_x from diesel and lean-gasoline engines.¹ NO_x traps collect engine-out NO_x during lean operation and treat it during short, rich operation cycles.² Fresh NO_x traps work very well but cannot sustain their high efficiency over the lifetimes of vehicles. This drop in efficiency is believed to be caused by aging due to (1) high-temperature operation and (2) sulfation-desulfation cycles necessary because of sulfur oxides in the emissions from the oxidation of sulfur in the fuel. In order to design a thermally durable NO_x trap, there is a need to understand the changes in the microstructures of materials that occur during various modes of operation (lean, rich, and lean-rich cycles). This information can form a basis for the selection and design of new NO_x trap materials that can resist the deterioration under normal operation.

The NO_x traps are derived from commercial three-way catalysts (TWCs) installed to treat emissions from engines

operating at stoichiometric air-fuel ratios. Therefore, the basic components of NO_x traps are identical to TWCs. The advanced version of a TWC is a two-layer system on a honeycomb substrate, with the inner layer based on Pt-alumina and the outer layer based on rhodium-ceria-zirconia. The NO_x traps derived from advanced TWCs are identical to them with the exception of high baria content (the upper limit being close to 20%) in the alumina layer. Thus the aging can lead to intermixing of layers, crystallization of baria-containing phases that are not good NO_x absorbers, and sintering of precious metals. The first goal of the project is to determine if one or all of microstructural changes take place and if these changes occur during lean, rich, or lean-rich cycles.

The tasks to achieve this goal are as follows:

- Complete microstructural characterization of fresh and thermally aged NO_x trap materials to determine the species formed as a result of aging.

- Complete microstructural characterization of fresh NO_x trap materials after exposure to lean conditions to determine the species formed during lean cycles.
- Complete microstructural characterization of fresh NO_x trap materials after exposure to rich conditions to determine the species formed during rich cycles.

The second goal of the project is to investigate and design new materials that can withstand NO_x trap operating conditions without undergoing detrimental structural changes. The results from the first goal will provide insights into changes that occur in NO_x trap materials at a microstructural level upon extended exposure to NO_x trap operating conditions, enabling the selection and design of materials for the second goal.

Results

A. Microstructural changes in supplier samples on aging under lean, rich, and stoichiometric conditions

A complete electron microscopic analysis of supplier catalyst aged under lean, rich, and stoichiometric conditions on a pulsator for lean gasoline conditions shows some interesting features.

- The fresh sample is a two-layer system on a honeycomb cordierite substrate. The inner layer is Pt/BaO-Al₂O₃ and the outer layer is CeO₂-ZrO₂. There are alumina islands in the CeO₂-ZrO₂ layer that contain some Ba. A dark field image of the CeO₂-ZrO₂ layer shows bright areas for the alumina islands and dark spots for segregated zirconia (Figure 1). This segregated zirconia is present only in fresh samples and is not seen in any of the aged samples. This suggests that segregated zirconia reacts with the CeO₂-ZrO₂ during aging. Since CeO₂-ZrO₂ forms under moderate conditions and crystallizes in a cubic fluorite phase regardless of ratio, the reaction of



Figure 1. Dark field image of CeO₂-ZrO₂ layer in fresh sample.

segregated ZrO₂ with CeO₂-ZrO₂ is not surprising.

- The dark field image of the BaO-Al₂O₃ layer shows a uniform distribution of Pt particles (Figure 2). In general, Pt particles are about 5 nm. There is no indication of Pt or Ba in the CeO₂-ZrO₂ layer.
- The two layers in lean aged samples remain intact. The segregated zirconia in the CeO₂-ZrO₂ layer, seen in the fresh sample, is no longer segregated. The representative Pt particles seen in the dark field image (Figure 3) have considerably increased in size compared with fresh samples. The partial migration of Ba from the BaO-Al₂O₃ layer to the CeO₂-ZrO₂ layer can be inferred from the electrodispersive spectroscopy of an area near the outer edge of the CeO₂-ZrO₂ layer.
- The microstructure of rich aged sample is identical to that of lean aged sample.
- The aging under stoichiometric conditions leads to partial migration of Ba from the BaO-Al₂O₃ layer to the CeO₂-ZrO₂ layer. The sintering of Pt particles also occurs, but the extent of sintering is smaller than under lean or rich conditions (Figure 4). [Note: The stoichiometric conditions refer to conditions under which the TWC operates in current gasoline-powered passenger vehicles.]

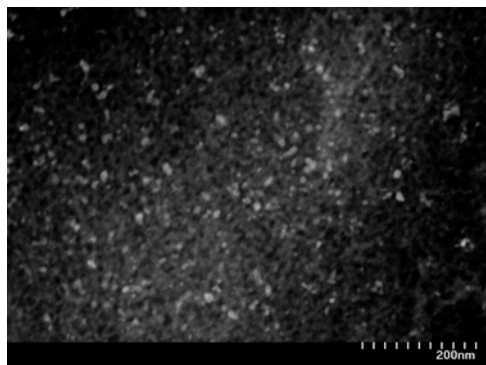


Figure 2. Dark field image of Pt/BaO-Al₂O₃ layer showing Pt particles in fresh sample.

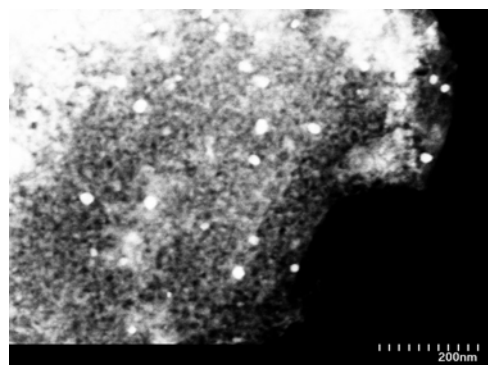


Figure 3. Dark field image of Pt/BaO-Al₂O₃ layer in lean aged sample.

Thus there are two pathways that can lead to reduced Pt–Ba oxide contact. The increase in Pt particle size due to sintering reduces the number of catalyst sites that are available and in contact with Ba oxide. The partial migration of Ba into CeO₂-ZrO₂ leads to reduced Ba in the alumina layer that can be in contact with or in close proximity to Pt. Both pathways occur during lean or rich aging of NO_x trap catalysts.

B. Model catalyst materials

The complexity of the lean NO_x trap system described warrants a complex model system that can be analyzed and evaluated in a laboratory. Improvements in the model system then can be implemented in a full-size catalyst that can be tested on a vehicle.

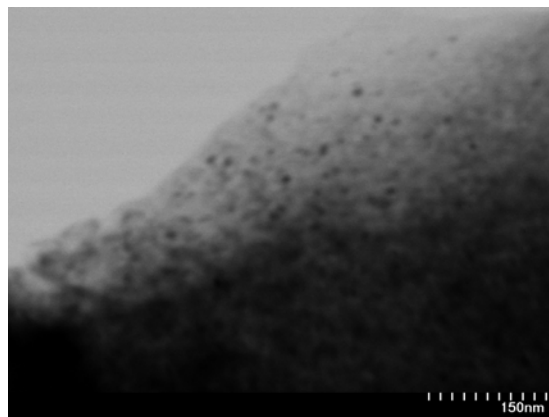


Figure 4. Dark field image of Pt/BaO-Al₂O₃ layer in stoichiometric aged sample.

While at Ford, the Oak Ridge National Laboratory principal investigator started addressing the thermal durability of NO_x trap materials. He found that a model system [10%CeO₂-ZrO₂-90%(2%La₂O₃-98%BaO.6Al₂O₃)] retains its beneficial surface properties even after thermal aging at 1050°C. This material can be prepared as follows:

1. Impregnation of Ba(NO₃)₃ on commercial high-surface-area alumina, pyrolysis, and sintering at 750°C.
2. Impregnation of the step 1 material with lanthanum nitrate, pyrolysis, and sintering at 750°C.
3. Ball-milling of the step 2 material with commercial high-surface area CeO₂-ZrO₂.

We impregnated this powder with 1% Pt and investigated Pt distribution on the powder. The electron micrograph shows that Pt particles are about 1 nm in size (Figure 5).

A second set of materials, Pt/BaO-Al₂O₃, was prepared by two different methods. In the first method, a sample of Pt-alumina was impregnated with a Ba compound and carefully pyrolyzed. In the second method, a sample of Pt-alumina was ball-milled with a Ba compound and then pyrolyzed. The

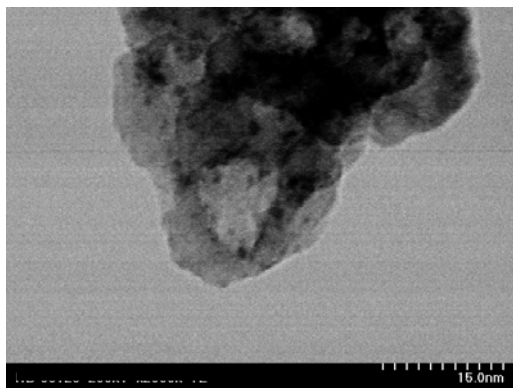


Figure 5. Dark field image of Pt/[10%CeO₂-ZrO₂-90%(3%La₂O₃-97%BaO.6Al₂O₃)].

samples have 2 wt % Pt and 18 wt % Ba. The X-ray powder diffraction patterns of the samples show sharp peaks due to the Ba carbonate, suggesting that the Ba oxide component had reacted with atmospheric CO₂. The broad diffraction peaks due to microcrystalline γ -alumina can also be seen.

Figure 6a shows typical morphologies of the as-impregnated Ba carbonate and alumina components. The long needles show energy-dispersive X-ray spectra (Figure 6b) consistent with BaCO₃ (as expected, based on XRD data), as shown in the computed spectrum for BaCO₃ in Figure 6c. The copper and aluminum peaks come from secondary excitation of a copper specimen grid and the adjacent alumina phase, respectively. Figure 6d shows the spectrum from the fine-grain structure, confirming the composition as alumina, with clear Pt peaks arising from the Pt loading as the catalytic species.

Figure 7 is a typical micrograph of the ball-milled Pt/Al₂O₃/baria material. The carbonate needles are effectively broken up, so there is a more intimate mixture of the Ba compound with the Pt/alumina material.

C. Ex-situ reactor

The existing ex-situ reactor needed to be completely redesigned for this project. The new schematics and design of the ex-situ reactor are shown in Figures 8 and 9,

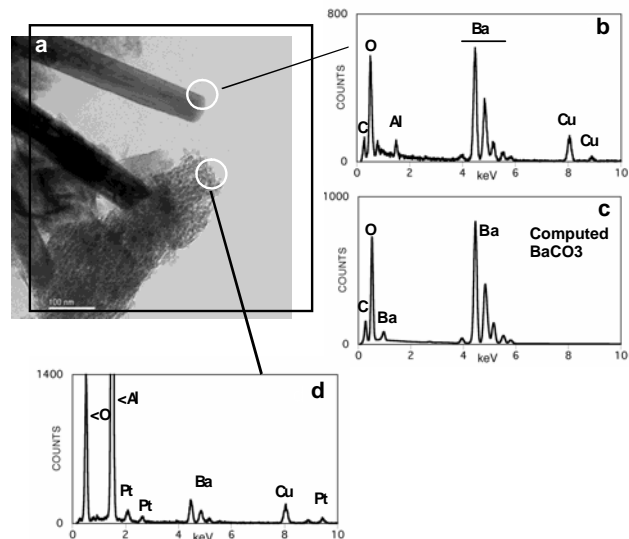


Figure 6. Pt/Al₂O₃ catalyst as impregnated with BaO. The needle structures are BaCO₃ phase, and the fine structure is the Pt/alumina phase. The copper peaks result from the specimen grid.

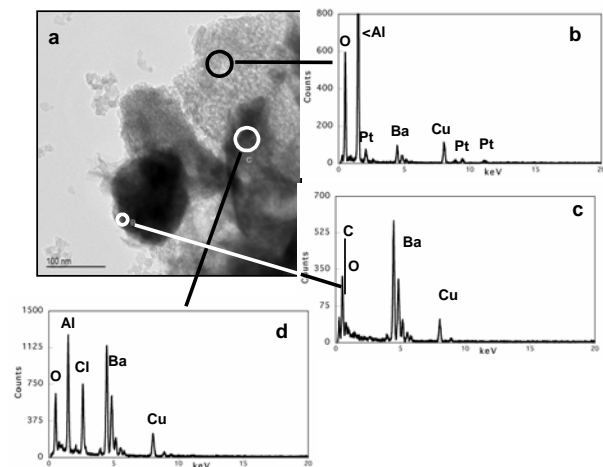


Figure 7. Ball-milled Pt/Al₂O₃/baria catalyst showing breakup of carbonate needles to give intimate mixture of fine-structured Pt/alumina phase and Ba carbonate. Copper results from the specimen grid, and the chlorine peak in three dimensions is most likely from residual chlorine from precursors. (Note energy scale change from Figure 6.)

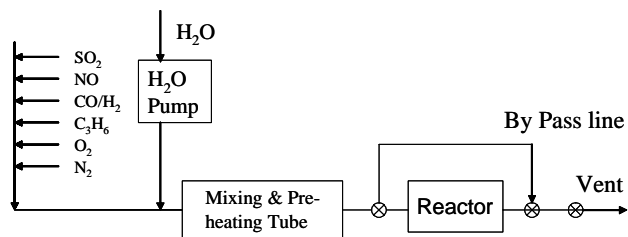


Figure 8. Schematics of the ex-situ reactor.



Figure 9. Ex-situ reactor for controlled atmosphere treatment of TEM samples.

respectively. The gas controller system and the water pump have been installed and calibrated for a total gas flow of 100cc/min.

Other Activities

The synthesis laboratory is now equipped to enable preparation of NO_x trap materials. Several items are on order for setting up a benchtop flow reactor in a laboratory at NTRC. A graduate student from the University of New Mexico is working with ORNL to support this project.

References

1. N. Miyoshi, S. Matsumoto, K. Katoh, T. Tanaka, J. Harada, N. Takahashi, K. Yokota, M. Sigiura, and K. Kasahra, "Development of New Concept Three-Way Catalyst for Automotive Lean-Burn Engines," SAE paper 95-0809, Society of Automotive Engineers.
2. N. Takahashi, H. Shinjoh, T. Iijima, T. Suzuki, K. Yamazaki, K. Yokota, H. Suzuki, N. Miyoshi, S. Matsumoto, T. Tanizawa, S. Tateishi, and K. Kasahara, "The New Concept 3-Way Catalyst for Automotive Lean-Burn Engine, NO_x Storage and Reduction Catalyst," *Catalysis Today*, **27**, 63–69 (1996).

F. Aftertreatment Catalyst Materials Research

*Matthew Henrichsen, Randy Stafford, and Paul McGinn**

Cummins, Inc.

1900 McKinley Ave.

Columbus, IN 47203

(812) 377-4170; fax: (812) 377-7226; e-mail: 377matthew.henrichsen@cummins.com

**Notre Dame University, South Bend, Indiana*

DOE Technology Development Area Specialist: Dr. Sidney Diamond

(202) 586-8032; fax: (202) 586-2476; e-mail: sid.diamond@ee.doe.gov

ORNL Technical Advisor: D. Ray Johnson

(865) 576-6832; fax: (865) 574-6098; e-mail: johnsondr@ornl.gov

Contractor: Oak Ridge National Laboratory, Oak Ridge, Tennessee

Prime Contract No: DE-AC05-00OR22725

Subcontractor: Cummins, Inc., Columbus, Indiana

Objectives

- Develop knowledge and tools necessary to satisfy the U.S. Environmental Protection Agency (EPA) 2007 and 2010 diesel emissions regulations while minimizing the total cost of ownership.

Approach

- Develop reactors and test methods for understanding the fundamental behavior of catalysts.
- Evaluate novel base metal oxide catalysts for oxidation of diesel soot with conventional and microwave heating.
- Improve understanding of sulfation and desulfation of commercial NO_x reduction catalysts through reactor studies.

Accomplishments

- Circumvented the limited ability of mass spectrometry to measure concentrations of gases with near-identical molecular weights, allowing measurement of, for example, CO in N₂.
- Developed a liquid hydrocarbon injector useable on a wide range of reactors.
- Designed a dedicated catalyst aging reactor.
- Designed and constructed a microwave-heated microreactor system.
- Developed a method for rapid automated screening of base metal oxide catalysts and used it to evaluate catalysts produced through combinatorial chemistry.

Future Direction

- Conduct sulfation and desulfation studies on commercial catalysts.
 - Compare catalyzed soot oxidation rates with conventional and microwave heating.
-

Introduction

The 2007 and 2010 EPA regulations on particulate and NO_x emissions from diesel engines are significantly lower than the current regulatory standards. These regulations are seen as aftertreatment-forcing by the diesel industry.

Though aftertreatment systems have been demonstrated that meet the 2007 emissions standards, more fundamental knowledge of the catalysts and the systems in which they operate is needed to optimize system performance and improve emissions performance with the lowest possible economic impact. Catalyst suppliers are commonly unwilling to allow third parties (such as national laboratories or academic institutions) to freely evaluate their proprietary catalyst formulations. We are developing the reactor systems and methods necessary to develop the fundamental knowledge of catalyst performance that we need for system optimization.

Catalysts commonly used for soot oxidation in catalyzed soot filters are based on platinum group metals and cerium oxides. The use of platinum group metals significantly increases the cost of catalyst systems. Base metal oxide catalysts, while typically less active than platinum group metal catalysts, are much less expensive. Oxidation activity has been reported at low temperatures with base metal oxides with both conventional and microwave heating.^{1,2} Because of the large potential impact on system cost, we are investigating the performance of base metal oxide catalysts.

Approach

To develop the tools necessary to develop a fundamental understanding of catalyst operation, we have pursued several paths. Of the many approaches, the three most significant are (1) a modification of Cummins' spatially resolved capillary-inlet mass spectrometer (SpaciMS) system³ that

allows resolution of species of similar molecular weights, (2) design of a reactor for aging of catalyst cores, and (3) design and construction of a microwave-heated reactor.

Novel base metal oxide catalysts were evaluated, in collaboration with Notre Dame University, using automated thermal gravimetric analysis (TGA) as a rapid screening tool to evaluate catalyst powders produced by combinatorial chemistry. This allows a large range of mixed oxides to be evaluated with a minimum of operator involvement. To extend this work to microwave-heated systems, a microwave-heated TGA was constructed.

Results

SpaciMS

Only a very sensitive and expensive mass spectrometer is capable of differentiating between molecules with masses that differ by a fraction of one atomic mass unit. In the reaction systems of interest to the diesel industry, molecule pairs that cannot be easily differentiated include N₂ and CO, NH₃ and H₂O, H₂S and ¹⁷O₂, and various hydrocarbons. However, the molecules of these confounded pairs have different chemical behaviors. By using a catalyst, the difference in chemical behavior can be used to separate the signals of the confounded species. For example, an oxidation catalyst can be used to convert CO to CO₂, which would allow easy separation of N₂ and CO.

In the SpaciMS system, the gas sample is drawn into the mass spectrometer through a small glass capillary. This capillary is a convenient substrate upon which the catalyst can be deposited. A micrograph of a catalyzed capillary is shown in Figure 1. The white material visible on the inner surface of the capillary is the catalyst layer. The same oxidation catalyst is also capable of differentiating between methane and other hydrocarbons (see Figure 2). By heating the capillary to a higher temperature, it would

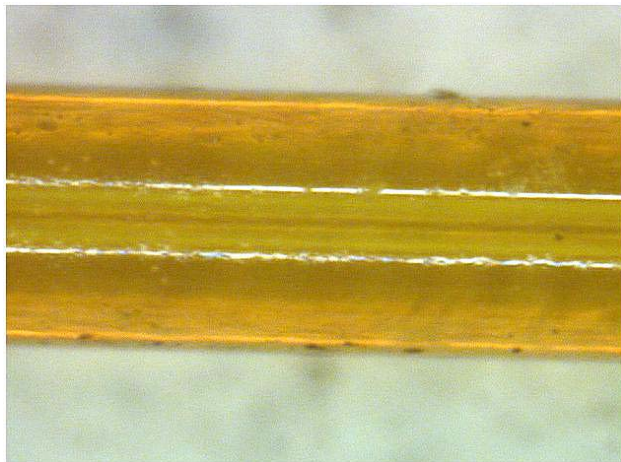


Figure 1. Capillary with an oxidation catalyst on the inner surface.

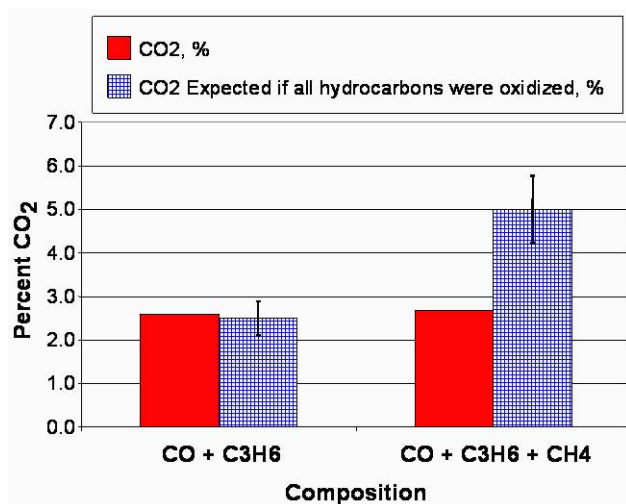


Figure 2. Combined CO and C₃H₆ oxidation compared with and without methane. The hatchmarked bars indicate the concentration of CO₂ expected if all CO and hydrocarbon were oxidized.

also be possible to completely oxidize the methane so that it would be converted to CO₂ and measured with the other hydrocarbons.

Dedicated Aging Reactor

Aging and deactivation of catalysts in use has a significant impact on catalyst performance. In order to accurately predict emissions performance over the lifetime of an aftertreatment system, aging must be understood. Aging catalysts behind engines

is an expensive proposition, and collection of statistically significant samples would be prohibitively expensive. Using performance reactors for this task is also time-consuming and greatly increases the number of performance reactors required to evaluate a catalyst formulation or deactivation mechanism.

To reduce the cost of validating catalyst formulations, a reactor capable of aging several specimens in parallel was designed (see Figure 3). The reactor is capable of exposing catalyst samples to high temperatures with controlled concentrations of water, catalyst poisons, and combustion products.

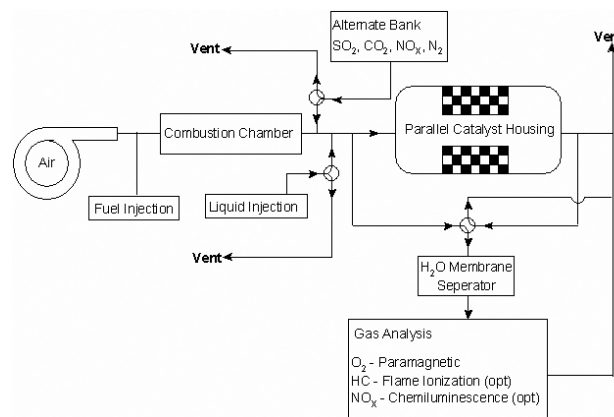


Figure 3. Schematic drawing of the catalyst aging reactor.

Microwave Reactor System

To quantify the impact of microwave heating on catalytic activity, a microwave reactor was developed. The microwave heating system, except for the portion immediately surrounding the reactor, has been described previously.⁴ A quartz reactor vessel is passed through a modified WR340 waveguide to provide heating. A drawing of the modified waveguide is shown in Figure 4. A moveable short and a 3-stub tuner are used to convert the traveling wave generated by the magnetron into a standing wave capable of being focused on the reactor. A multiprobe optical fiber temperature

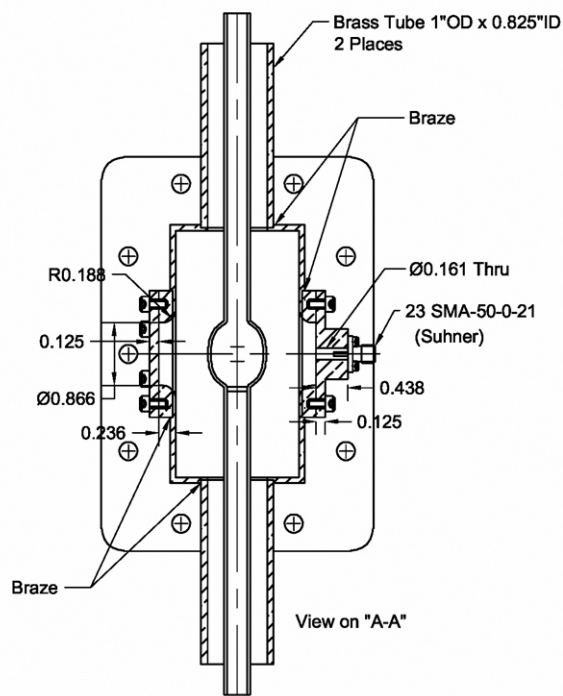


Figure 4. Detailed schematic of the microwave reactor cavity.

measurement system is used to allow precise temperature measurement inside the reactor bed without distorting the microwave field.

Specimens heated in the microwave reactor consist of catalyst, soot, and quartz chips. The quartz chips help to reduce the tendency toward thermal runaway in both microwave heating and soot oxidation by increasing the effective specimen thermal mass. When microwave power is applied with gas flowing through the reactor, a temperature gradient develops in the bed. Although this temperature gradient is unavoidable, it is predictable; and kinetic evaluations can be corrected for its effect on reaction rates. A mass spectrometer is used to measure the combustion products coming out of the catalyst bed.

Catalyzed soot oxidation has been measured in the microwave reactor but has not yet been compared with similar data from a conventionally heated reactor.

Screening of Base Metal Oxide Catalysts

Mixed base metal oxide catalysts have been prepared using a broad range of base metals. The basic method has been reported in detail elsewhere.⁵ The oxidation performance of several mixtures was examined using TGA. The results of several mixtures are shown in Figure 5.

Oxidation rates are strongly affected by the contact between the soot and the catalyst material. When they are more intimately mixed (tight contact), as with a mortar and pestle, the oxidation rate is higher for many catalysts. Typically, loose-contact oxidation rates match tight-contact oxidation rates when a liquid forms (e.g., when the catalyst melts) or when there is a vapor phase intermediate in the reaction (e.g., NO₂ in platinum-catalyzed low-temperature soot oxidation, or volatilization of chloride salts). Contact between soot and catalyst in diesel particulate filters is similar to “loose” contact.

In the results shown in Figure 5, the oxidation rate is controlled primarily by the second component (A, B, C, D, or E) rather than the first metal oxide component (X or Y). Additionally, the impact of the second component is largely independent of the relative proportion of the two components. The observed low oxidation temperatures near 350°C are low enough to be interesting, but the similarity of the temperatures for

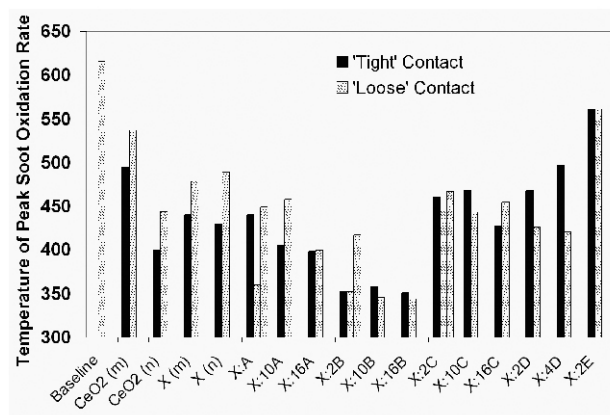


Figure 5. Relative peak oxidation rates with several catalyst compositions.

loose and tight contact indicate that solid-solid catalysis is not the primary mechanism.

Microwave TGA

To expand the base metal catalyst screening work to microwave heating, a microwave TGA system was constructed. The system was designed around a commercial microwave oven. Figure 6 shows a sketch of the equipment.

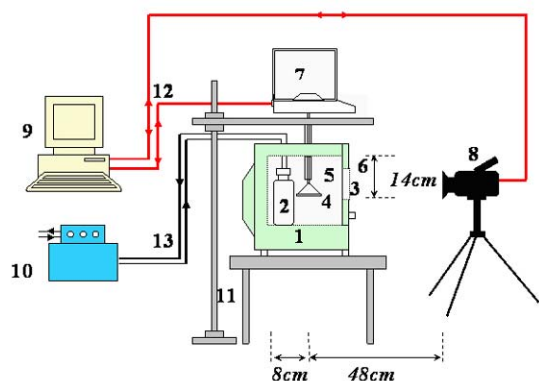


Figure 6. Schematic of the microwave TGA. (1) Sharp 2100W/R-25JT microwave, (2) cooling water reservoir, (3) CaF_2 single crystal window, (4) quartz sample holder, (5) quartz sleeve and hanging rod, (6) modified microwave door, (7) GR-120 AD balance, (8) Prism DS IR camera, (9) computer, (10) pump, (11) steel stand, (12) input and output cables connecting computer/camera and computer/balance, (13) plastic tubing for input and output water.

Temperature measurement is performed using an infrared camera (Flir Prism DS) through a hole in the door suitably fitted with a microwave shield. An infrared camera is used to avoid the use of a thermocouple, which would distort the microwave fields. The camera is used to take a picture of the sample periodically (e.g., every 2 seconds), which is saved for later analysis to determine temperature as a function of time.

To reduce vibration of the balance, it rests on a steel frame that does not contact the microwave. The quartz specimen basket

is suspended from the balance by a quartz rod. The quartz rod is shielded by a quartz sleeve to minimize swaying due to air circulation in the microwave oven. To assist in heating the specimen, a small microwave-absorbing SiC susceptor is placed under the specimen in the bottom of the quartz specimen basket. A plastic bottle of water is placed inside the microwave cavity to serve as a load and to help control the specimen heating rate.

An example of the data obtained for heating of just Degussa carbon soot (after necessary temperature and weight corrections) is shown in Figure 7, along with superimposed data from the conventional TGA. This curve was obtained with ~4 minutes of heating in the microwave field. As shown in the curve, noticeable soot oxidation begins at about 600°C, as is seen in our conventional TGA measurements (obtained at a heating rate of 20°C/min in 100 ml/min air flow). The weight of the material used in these experiments is much greater than in conventional TGA because of the reduced sensitivity of the balance. The comparison shows that the microwave TGA data can be reliable.

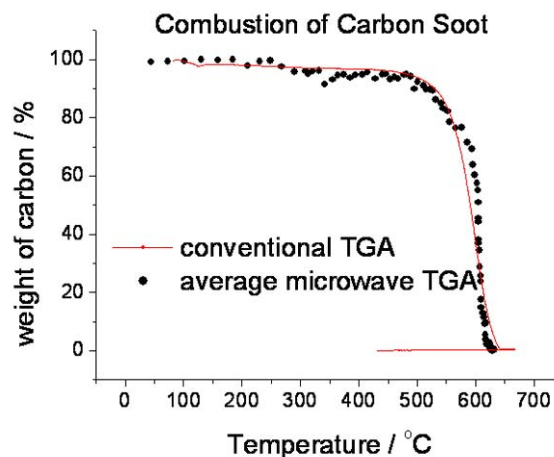


Figure 7. Microwave and conventional thermal gravimetric analysis curves for combustion of carbon soot in the air.

Summary and Conclusions

It is possible, with a low-resolution mass spectrometer, to differentiate between molecules with similar molecular weights by differences in their chemical behavior. This approach will be useful in evaluating gas-phase composition in catalysts operating both in reactors and on engines.

A dedicated aging reactor and a microwave reactor were designed, and the microwave reactor was constructed. Although the reactor bed had a measurable temperature gradient during operation, it was predictable. Soot was catalytically oxidized in the microwave reactor. A detailed comparison of microwave and conventionally heated reaction rates will be completed in the near future.

A wide variety of mixed-oxide catalyst materials were produced, and their catalytic activity was evaluated using TGA. A microwave TGA was constructed that will allow reliable evaluation of microwave catalytic activity. Catalyst compositions were found that lowered the peak soot oxidation temperature to ~350°C with conventional heating. Although the low oxidation temperature is significant, that catalyst formulation may not be sufficiently stable in a diesel environment. However, a reduction in regeneration temperature of that magnitude would reduce the regeneration fuel penalty and increase system life.

References

1. J. P. A. Neeft, M. Makkee, and J. A. Moulijn, "Catalysts for the Oxidation of Soot from Diesel Exhaust Gases. 1. An Exploratory Study," *Applied Catalysis B-Environmental*, **8**, 57–78 (1996).

2. M. Fang, J. Ma, P. Li, N. T. Lau, B. Zhu, and X. Lu, "Microwave-Assisted Catalytic Combustion of Diesel Soot," *Applied Catalysis A: General*, **159**, 211–228 (1997).

3. N. W. Currier, M. J. Cunningham, W. P. Partridge, J. M. Storey, S. A. Lewis, R. W. Smithwick, and G. L. DeVault, "Exhaust Aftertreatment, Gas Phase Measurements in situ," presented at DEER 2000: 6th Diesel Engine Emissions Reduction Workshop, August 20–24, 2000, to be published in the proceedings.

4. M. Henrichsen and S. Popuri, "Development of a Microwave-Assisted Particulate Filter," presented at DEER 2001: Seventh Diesel Engine Emissions Reduction Workshop, August 5–9, 2001, to be published in the proceedings.

5. H. M. Reichenbach, H. An, and P. J. McGinn, "Combinatorial Synthesis and Characterization of Mixed Metal Oxides for Soot Combustion," *Applied Catalysis B: Environmental*, **44**, 347–354 (2003).